USGS
science for a changing world

In cooperation with the California Department of Water Resources, the California Department of Parks and Recreation, and the Nevada Irrigation District

Quantifying Erosion Rates by Using Terrestrial Laser Scanning at Malakoff Diggins State Historic Park, Nevada County, California, 2014–17

Open-File Report 2019–1124

U.S. Department of the Interior
U.S. Geological Survey

Front cover: FARO laser scanner at Malakoff Diggins State Historic Park study site 5. View to the west. Photograph taken by James F. Howle, August 23, 2017.

Back cover: U.S. Geological Survey scientist collecting sediment sample at Malakoff Diggins State Historic Park study site 4. View to the west. Photograph taken by A.J. Ward, June 3, 2015.

Quantifying Erosion Rates by Using Terrestrial Laser Scanning at Malakoff Diggins State Historic Park, Nevada County, California, 2014–17

By James F. Howle, Charles N. Alpers, Alfred J. Ward, Sandra Bond, and Jennifer A. Curtis

In cooperation with the California Department of Water Resources, the California Department of Parks and Recreation, and the Nevada Irrigation District

Open-File Report 2019–1124

U.S. Department of the Interior
U.S. Geological Survey

U.S. Department of the Interior
DAVID BERNHARDT, Secretary

U.S. Geological Survey
James F. Reilly II, Director

U.S. Geological Survey, Reston, Virginia: 2019

Suggested citation:
Howle, J.F., Alpers, C.N., Ward, A.J., Bond, S., and Curtis, J.A., 2019, Quantifying erosion rates by using terrestrial laser scanning at Malakoff Diggins State Historic Park, Nevada County, California, 2014–17: U.S. Geological Survey Open-File Report 2019–1124, 39 p., https://doi.org/10.3133/ofr20191124.

Associated data for this publication:
Howle, J.F., 2019, Terrestrial laser scanning data from Malakoff Diggins State Historic Park, Nevada County, California, 2014–17: U.S. Geological Survey data release, https://doi.org/10.5066/P9H3VNSN.

ISSN 2331-1258 (online)

Acknowledgments

Funding for this project was provided by the California Department of Water Resources through its Integrated Regional Water Management grant program. An Integrated Regional Water Management grant for the Cosumnes, American, Bear, and Yuba Rivers region was managed by The Sierra Fund. Funds were provided to the U.S. Geological Survey through a cooperative agreement with the Nevada (County) Irrigation District. Project management at The Sierra Fund was done by Beth Bordner and Carrie Monohan and at the Nevada Irrigation District by Tim Crough, Greg Jones, and Neysa King. Permits and logistical support were provided by the California Department of Parks and Recreation (State Parks). Individuals at California State Parks who assisted with this work included Syd Brown, Matt Green, Denise Jaffke, Dan Lubin, Dan Millsap, Tamara Sasaki, Cyndie Walck, and Dan Youngren. Field assistance was provided by Nick Graham (California State University, Chico, and U.S. Geological Survey), George Valente (The Sierra Fund), Steve Schmitt (U.S. Geological Survey), and several other students from California State University, Chico.

Contents

Figures

Tables

Conversion Factors

International System of Units to U.S. customary units

Multiply	By	To obtain
	Length	
centimeter (cm)	0.3937	inch (in.)
millimeter (mm)	0.03937	inch (in.)
meter (m)	3.281	foot (ft)
kilometer (km)	0.6214	mile (mi)
meter (m)	1.094	yard (yd)
	Area	
square meter (m^2)	10.76	square foot (ft^2)
square centimeter (cm^2)	0.1550	square inch ($in.^2$)
	Volume	
cubic meter (m^3)	35.31	cubic foot (ft^3)
	Mass	
kilogram (kg)	2.205	pound avoirdupois (lb)

Abbreviations and Symbols

±	plus or minus
1-SD	one-standard-deviation
2-D	two-dimensional
2-SD	two-standard-deviation
3-D	three-dimensional
lidar	light detection and ranging
RMSE	root-mean-squared error
TIN	triangulated irregular network
TLS	terrestrial laser scanning
USGS	U.S. Geological Survey

Note that selected technical terms are defined in the Glossary. These terms are indicated in **bold font** the first time they appear in the main body of the report.

Quantifying Erosion Rates by Using Terrestrial Laser Scanning at Malakoff Diggins State Historic Park, Nevada County, California, 2014–17

By James F. Howle, Charles N. Alpers, Alfred J. Ward, Sandra Bond, and Jennifer A. Curtis

Abstract

The abandoned hydraulic mine pit at Malakoff Diggins near Grass Valley, California, can produce large volumes of eroded sediment transportable by storm runoff. Sediment-laden water discharged from the pit is a major source of heavy metals to Humbug Creek and the South Yuba River. To develop a comprehensive sediment budget for the Malakoff Diggins mine pit and identify sources of sediment and metals within the pit that can become entrained as suspended sediment in runoff discharged from the pit, the U.S. Geological Survey, working in cooperation with the California Department of Water Resources, the California Department of Parks and Recreation, and the Nevada Irrigation District, used terrestrial laser scanning technology to quantify eroded volumes and erosion rates of sedimentary units exposed in the pit walls. The results for eroded volumes and rates reported here are part one of a three-part study.

High-resolution terrestrial laser scanning surveys were repeated annually from 2014 through 2017, including before and after dry and wet winters, measuring centimeter-scale topographic changes to quantify the volume of sediment eroded from outcrops at Malakoff Diggins State Historic Park, located on the western slope of the northern Sierra Nevada about 17 kilometers northeast of Grass Valley, California. Terrestrial laser scanning enabled construction of three-dimensional maps of the complex outcrop surfaces, which could not be mapped non-destructively or in sufficient detail with traditional surveying techniques. Net eroded volumes from discrete sedimentary units were calculated at four study sites (numbered 1, 2, 4, and 5) throughout the mine pit for the December 2014 to August 2017 period.

Net eroded volumes at the four study sites during the 32-month study ranged from 288 plus or minus (±) 13 cubic meters (m^3) of sediment at site 1 to 8,517±145 m^3 at site 4. Annual erosion rates at the four study sites ranged from 0.06±0.01 cubic meters per square meter per year ($m^3/m^2/yr$) at site 4 to 0.14±0.01 $m^3/m^2/yr$ at site 2. The total net eroded volume documented with terrestrial laser scanning at all four study sites from December 2014 to August 2017 was 12,934±334 m^3 of sediment, and the average annual erosion rate for the four study sites was 0.10±0.04 $m^3/m^2/yr$.

Maps of horizontal retreat indicate that a variety of erosional processes were responsible for the eroded sediment volume. These included areally broad and smaller-scale processes such as persistent dry ravel, periodic sheet wash, and frost heave and more localized and larger-scale processes such as coalescing rill and gully erosion, debris flows, rotational landslides, and block-fall failures.

Introduction

Malakoff Diggins State Historic Park, located on the western slope of the northern Sierra Nevada about 17 kilometers (km) northeast of Grass Valley, California (fig. 1), was one of the largest **hydraulic gold mines** in California. The abandoned hydraulic mine pit at Malakoff Diggins is approximately 2 km long, up to 1 km wide, and 120 meters (m) deep in places (fig. 2). The Malakoff Diggins pit exhibits dissected badland topography (fig. 3), and during rainfall-runoff events this landscape can produce large volumes of sediment that collect in Diggins Pond. At higher pond stages the sediment-laden water in Diggins Pond drains through the Hiller Tunnel into Diggins Creek and eventually into Humbug Creek (figs. 1, 2). The pit represents the primary source of sediment and heavy metals to Humbug Creek and an important source to the South Yuba River (Fleck and others, 2011; Marvin-DiPasquale and others, 2011). Humbug Creek is listed under Section 303(d) of the Clean Water Act as impaired for sedimentation/siltation, pH, and concentrations of heavy metals including chromium (Cr), copper (Cu), iron (Fe), mercury (Hg), and zinc (Zn; California State Water Resources Control Board, 2017). A 39-mile reach of the South Yuba River became a state-designated Wild and Scenic River in 1999 (State of California, 2019).

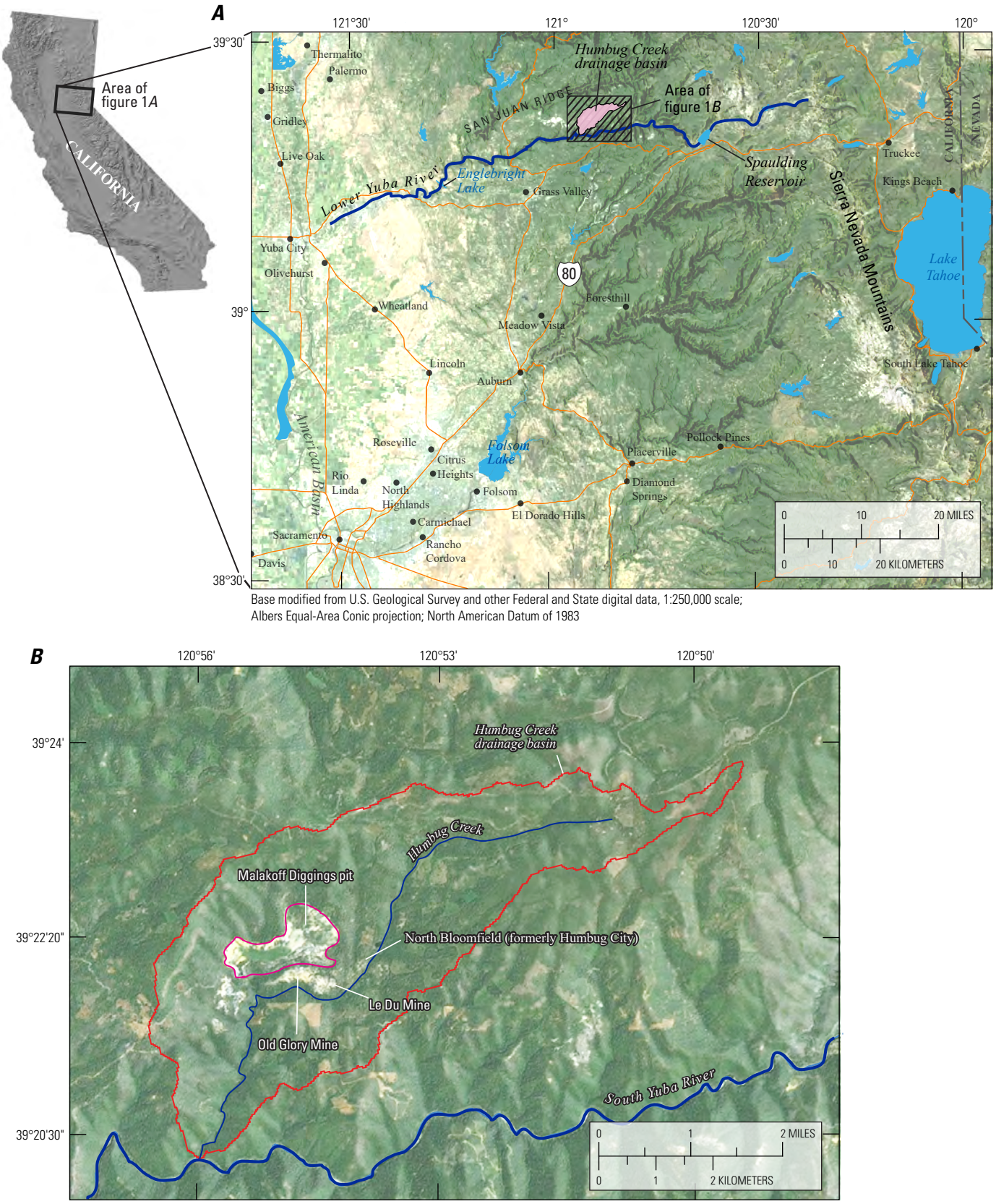

Figure 1. Areas discussed in the text: *A*, the Humbug Creek drainage basin and the South Yuba River; and *B*, the Humbug Creek drainage basin and Malakoff Diggings mine pit in the northern Sierra Nevada, California.

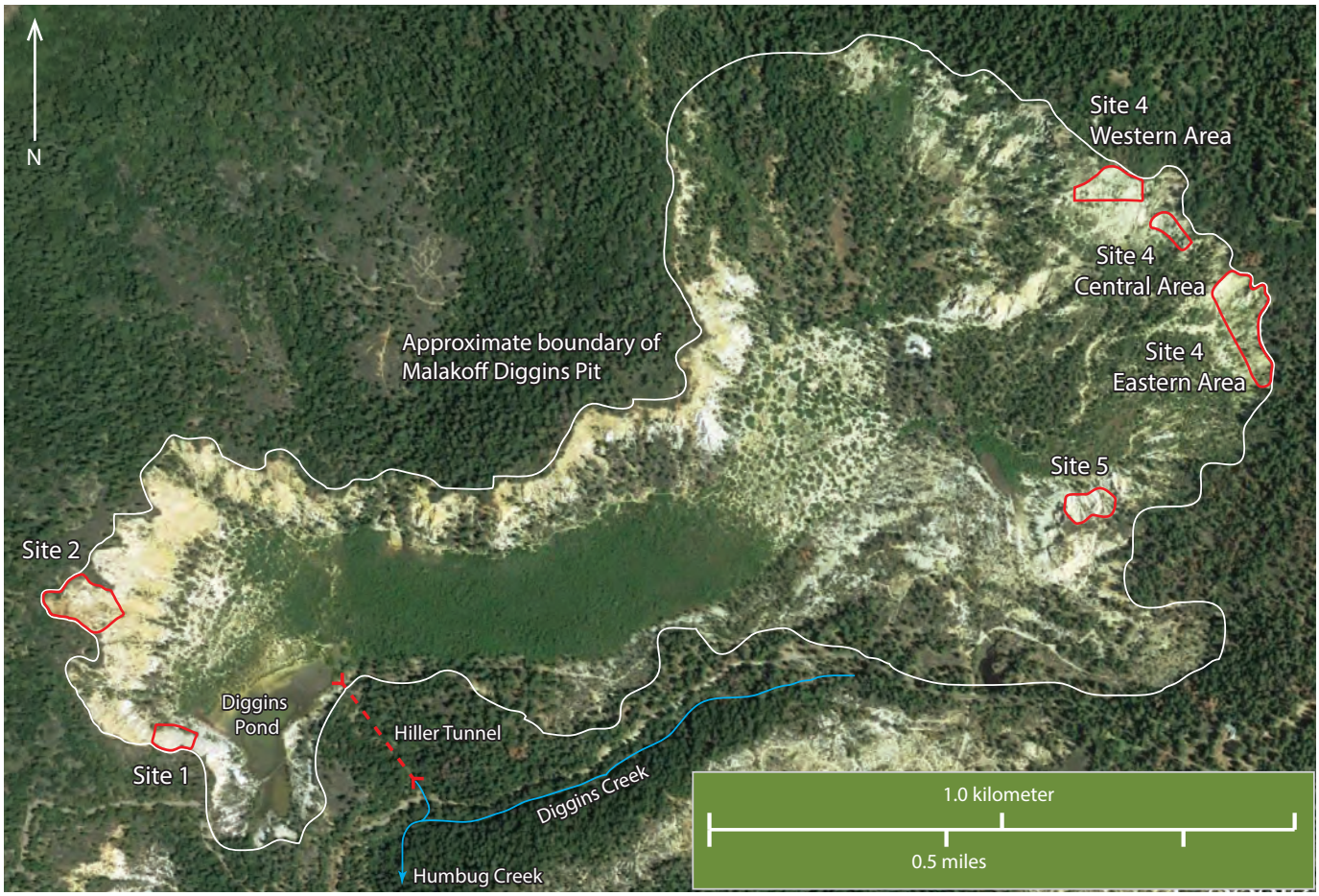

Figure 2. Malakoff Diggins mine pit and the locations of study sites, Diggins Pond, and the Hiller Tunnel.

Numerous sedimentary units are exposed in the pit walls (fig. 3); each having unique characteristics based on grain size, color, and geomorphic expression (slope angle; Curtis, 2017). The units display varying susceptibility to erosion caused by differences in grain size, compaction, and cementation. The finer-grained units typically are exposed in lower-angle, 'slope'-forming layers, whereas the coarser-grained units typically create steeper, 'cliff'-forming layers. Cassel and Graham (2011) documented four sets of alternating fine-grained and coarse-grained layers in the pit walls. Highest concentrations of the heavy-metal elements of concern are found comingled with the fine-grained silt- and clay-size (less than 0.063 millimeters) sediment fraction (Fleck and others, 2011). Although fine-grained units presumably contribute a large proportion of the overall suspended-sediment and heavy-metal load to the surface-water discharge from the pit, coarser-grained units can also have significant silt- and clay-size fractions (Ward and others, 2019).

In cooperation with the California Department of Water Resources (DWR), California Department of Parks and Recreation (State Parks), and the Nevada Irrigation District, the U.S. Geological Survey (USGS) initiated a multi-year study to contribute quantitative data toward the development of a comprehensive sediment budget for the Malakoff Diggins mine pit. The overall goal of the study was to help identify sources of sediment and metals within the pit that yield the suspended sediment discharged from the pit into Humbug Creek. The specific objectives of the broader study are (1) to quantify the eroded volumes and erosion rates of sedimentary units exposed in the pit walls using high-resolution, ground-based (terrestrial) laser scanning technology (this study); (2) to characterize the grain-size distribution, mineralogy, and geochemistry of the sedimentary units within the Malakoff Diggins mine pit; and (3) to characterize the mineralogy and chemical constituents of suspended sediment being transported from the Malakoff Diggins mine pit to Humbug Creek. Results from parts 2 and 3 of the investigation are published separately (Ward and others, 2019). The erosion-rate information from this report combined with data on grain-size distribution, mineralogy, and geochemistry of the various sedimentary units will be used to test hypotheses regarding the sources of sediment and metals within the pit and the suspended sediment discharged from Hiller Tunnel.

Figure 3. Badland topography of the Malakoff Diggins mine pit, featuring active erosion and sediment transport to the pit floor (in background). The view is looking southwest from the northeastern rim of pit; the foreground shows a landslide head scarp at the eastern area of study site 4. The photograph was taken February 14, 2013.

Terrestrial laser scanning (TLS), also known as ground-based **lidar** (light detection and ranging), is a remote-sensing technology that can collect high-resolution (centimeter-scale), three-dimensional (3-D) measurements of the land surface that cannot be achieved with traditional surveying techniques (Heritage and Large, 2009). A laser scanner emits pulses of near-infrared laser light which are timed to measure the distance (range) from the laser scanner to the reflecting surface. Laser ranges are combined with angular orientation data to generate a dense and detailed set of points (x, y, and z locations of individual laser returns) referred to as a **point cloud**. The non-destructive measuring of the surface of the sedimentary units on repeat occasions and the sub-centimeter resolution of the point cloud allows for a spatially detailed assessment of topographic change and a quantitative measurement of the volume of erosion (or deposition) between data-collection events (Howle and others, 2019).

Four sequential TLS surveys of the four study sites (sites 1, 2, 4, and 5; fig. 2) were conducted during a 32-month period. Site 3, in the north central part of the pit (not shown on fig. 2), was not surveyed because of access and logistical issues, but was sampled for parts 2 and 3 of the investigation (Ward and others, 2019). Each survey at all four study sites was composed of multiple lidar scans collected from different vantages that were combined into a composite 3-D point cloud. At all four study sites, the sequential surveys were co-registered or 'aligned' into a common and site-specific reference frame so that volumetric comparisons between surveys could be made. At each study site, sedimentary units were differentiated based on grain size, color, compaction, cementation, and slope angle. The various sedimentary units were mapped on the lidar point clouds and individually isolated for volumetric change analysis. The volumetric differences between surveys quantify the erosional or depositional volume change of each sedimentary unit.

Purpose and Scope

The purpose of this report is to document the methods used and the volume of eroded sediment, as well as the rate of erosion, for 19 sedimentary units at 4 study sites in the Malakoff Diggins mine pit from December 2014 to August 2017. The results of this study will be combined with laboratory determination of grain-size distribution, mineralogy, and geochemistry of the various sedimentary units (Ward and others, 2019) to identify sources of sediment and metals within the pit that yield the suspended sediment discharged from the pit through the Hiller Tunnel. Results from this investigation can be used by the State of California to facilitate the design of an effective sediment and heavy-metal abatement program for water discharged into Humbug Creek and to determine whether stabilization is needed of sediment source areas in the Malakoff Diggins pit.

Methods

This section contains information on the methods of TLS data collection, point-cloud alignment, volumetric calculations, and planimetric area measurement of the sedimentary units. A description of the survey alignment error is also included.

Terrestrial Laser Scanning Data Collection

Terrestrial laser scanning data were collected on December 7–10, 2014; October 21–23, 2015; October 18–20, 2016; and August 22–24, 2017. At sites 1, 2, and 5 (fig. 2), a FARO Focus3D laser scanner (model S-120; FARO Technologies, Lake Mary, Florida) was used for the baseline survey during December 2014. For all subsequent surveys at sites 1, 2, and 5, a FARO Focus3D model X-330 scanner was used. Laser returns from both models of FARO scanners have a positional accuracy of plus or minus (±) 1.0 millimeter (mm) at a distance of 50 m (per manufacturer specifications), which was achieved by averaging the return of six laser pulses to determine the x, y, and z location of each recorded point. Points greater than 50 m from the scanner origin were not used in this study because those points would decrease the accuracy of the data. The FARO scanner was mounted on a standard survey tripod and automatically rotated about the vertical axis, collecting a full, 360-degree point cloud, except for a 60-degree-wide cone directly beneath the scanner. A pre-set laser-spot spacing of 6.7 mm at a distance 10 m from the scanner origin was used for all scans. At a distance of 50 m from the scanner origin, the average data density from a single scan was approximately 920 points per square meter (m^2), which is equivalent to a laser-spot spacing of approximately 30 mm. Where adjacent scans overlap, at a distance of 50 m from the scanner origin, the data density was greater by a factor of approximately two. The 360-degree field of view afforded by the ‘orbital’ FARO laser scanners was ideal for imaging the amphitheater topography of sites 1, 2, and 5 where the exposed sedimentary units were generally less than 50 m from the scanner origin. However, site 4 (fig. 2) encompassed a considerably larger area, which was not well suited for the near-field FARO scanner.

To image the approximately 0.5-km-wide area of site 4 efficiently, a long-range Optech ILRIS 36D laser scanner (Optech Inc., West Henrietta, New York) was utilized. The laser returns from the Optech scanner have a positional accuracy of plus or minus 4 mm at a distance of 100 m (according to manufacturer specifications). The site 4 outcrops ranged from approximately 400 m from the scanner in the eastern area to approximately 550 m in the western area, which yields positional accuracies of laser returns between plus or minus 16 mm to 22 mm, respectively. The laser-spot spacing was set to 20 mm for each cliff area, which yielded an average data density of approximately 2,500 points per square meter across the cliffs. Small areas of the cliff that surround 0.45-m-diameter alignment spheres, described later in this section, were defined to increase the data density of those areas to a laser-spot spacing of 10 mm. During each survey of site 4, the Optech laser scanner was deployed from atop the cliff on the west and east sides of site 5 (fig. 2), approximately 105 m apart. The stereo perspective of the two scanning locations helped minimize data shadowing, described later in this section, and increased the data density to approximately 5,000 points per square meter across the cliffs.

Point-Cloud Alignment

The construction of various monuments used to mount alignment and reference spheres is described in this section. Also discussed are the methods used to align or combine multiple scans in a given survey, the alignment of sequential surveys, and the quantitative assessment of the quality of alignments.

Alignment Spheres

To align individual scans collected during the same survey (that is, to combine the scans into a common x, y, and z reference frame), the FARO system utilizes spheres of 0.2- and 0.23-m diameter placed throughout the scan area (fig. 4). Adjacent scans typically had five to six spheres common to both scans that were used for alignment. Some alignment spheres were positioned temporarily on tripods, whereas other spheres were attached magnetically to monuments (fig. 4). The monuments were positioned along the periphery of the study sites to be in the line of sight of the laser scanner, and where possible, they were also established in the interior of the scanned study site. Monuments were set by several methods. Trees ranging in diameter from 0.3 to 1.2 m were used to mount the spheres by screwing magnetic mounts into tree trunks (fig. 4). Other monuments were constructed by digging holes, approximately 0.3 m wide and 0.5 m deep, into the alluvium. Then, 1.2 m long, 16-mm-diameter sections of threaded steel rod were driven into the alluvium at the center of the holes until 0.2 m of rod was left exposed above the ground surface. Each hole was backfilled to the land surface with about 30 kilograms (kg) of concrete. Approximately 0.15 m of the protruding rod was cased with 0.1-m-diameter polyvinyl chloride (PVC) pipe and filled with concrete, leaving about 5 centimeters (cm) of threaded rod exposed. Magnetic sphere mounts were then attached permanently to the threaded rod. This same construction method was also used for reference-sphere monuments, discussed in the next paragraph, except the threaded rod was left exposed so that removable 0.45-m-diameter spheres could be screwed onto the monument prior to scanning.

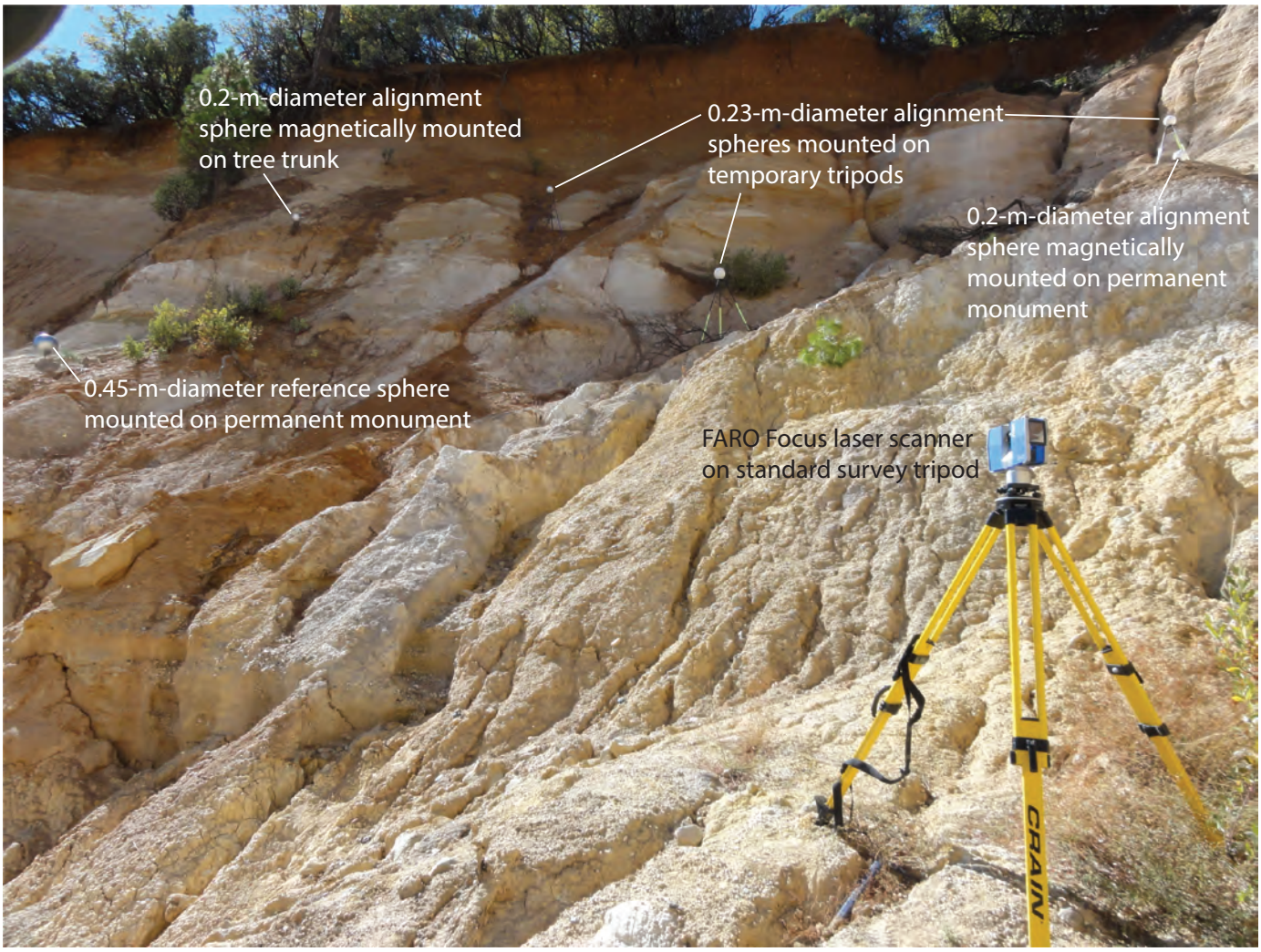

Figure 4. Tripod-mounted FARO laser scanner, alignment spheres, and reference spheres at Malakoff Diggins study site 2. The photograph was taken October 21, 2015.

Reference Spheres

The alignment quality of sequential TLS surveys was assessed quantitatively using an independent set of reference spheres at locations along the periphery of the study sites. Prior to scanning, 0.45-m-diameter reference spheres (dedicated to specific monuments) were screwed onto the stable monuments until the spheres were against the threaded rod. Linear reference marks on the spheres and rods were aligned so that each sphere could be reoriented on the corresponding monument to within 3 mm.

Alignment of Multiple Scans in a Survey

The alignment of scans for surveys at sites 1, 2, and 5 was accomplished using the software package SCENE (version 5.5.3.16, FARO Technologies, Lake Mary, Florida). For each scan in a survey, the SCENE software automatically identified the 0.2-m and 0.23-m-diameter alignment spheres (fig. 4) and determined their relative positions. The SCENE software then locked the position of the scan that had the greatest number of alignment spheres, while the remaining scans were rotated and translated until the spheres were best-fit in 3-D space relative to the locked scan.

To assess the quality of the alignment, the SCENE software also calculated a 1-standard-deviation (1-SD) error of the alignment. This error was computed from the spatial variations of the alignment-sphere center points for each unlocked scan relative to the locked scan.

At site 1, two scans approximately 20 m apart were made in all four surveys. The 1-SD error of the scan alignments for all surveys (2014–17) was on average (arithmetic mean) ±1.3 mm (±1.4 mm for the 2014 baseline survey, ±0.8 mm for the 2015 survey, ±1.2 mm for the 2016 survey, and ±1.9 mm for the 2017 survey). At site 2, six scans were required to fully image the topography and the average 1-SD alignment error for all surveys at this site was ±1.7 mm (±1.4 mm for the baseline survey, ±1.3 mm for the 2015 survey, ±1.0 mm for the 2016 survey, and ±3.2 mm for the 2017 survey). At site 5, five scans were conducted in all surveys and the average 1-SD alignment error was ±1.3 mm (±1.6 mm for the baseline survey, ±1.0 mm for the 2015 survey, ±1.0 mm for the 2016 survey, and ±1.5 mm for the 2017 survey).

The four annual surveys at site 4, which were scanned with the long-range Optech instrument, were composed of overlapping scans (nearly 100 percent of overlap) collected from two vantages approximately 105 m apart. The two scans were aligned or combined into a composite point cloud by using the PolyWorks® software package (version 12.0.15, InnovMetric Software Inc., Quebec City, Quebec, Canada). The initial alignment of the two scans was a manual procedure where both scans were viewed from the same perspective on dual computer monitors. Pairs of common points (such as distinct features on the outcrop surfaces) in each scan were identified, and the software then translated the coordinate system of one scan to the other. This initial placement typically produced alignments within plus or minus 10 cm. The decimeter-scale misalignment (from the initial manual placement) was automatically corrected with an iterative algorithm that computed an optimal alignment by minimizing the distance between the 3-D point clouds of the outcrop surfaces in the two overlapping scans. Through a series of rotations and translations, the overlapping scans were adjusted until a user-defined convergence (for this study 1 cm) between the two scans was achieved. For the 2014 survey, the 1-SD alignment error of the overlapping scans was 1.8 cm and for the 2017 survey, the 1-SD alignment error was 2.0 cm. These 1-SD alignment errors are approximately equivalent to the previously discussed positional accuracy of the laser returns and the laser-spot spacing.

Alignment of Sequential Surveys

To use the sequential surveys to calculate volumes of erosion or deposition there must be stable and common features in each survey so that the surveys can be aligned or co-registered to the same x, y, and z coordinate system. This study utilized the previously described monuments with attached alignment spheres that were spread around the study site to co-register the sequential surveys.

After the scans for a given survey were aligned, sphere center points were defined from the point clouds of the monument-mounted alignment and reference spheres using the PolyWorks® software package. The spherical point clouds were isolated in a 3-D environment and modeled as perfect spheres of a known radius (example in Howle and others, 2016). The modeled alignment and reference spheres were defined by thousands of points. From these statistically significant “best-fit” spheres, the center points were mathematically derived as unique (x, y, and z) points in 3-D space at sub-millimeter resolution (Howle and others, 2016; 2019).

The process of defining sphere center points was repeated for all of the monument-mounted alignment spheres in each survey. The alignment sphere center points for each survey had the same spatial (geometric) relation, but the x, y, and z coordinate systems differed because the laser scanner positions were slightly different during each survey. The alignment was accomplished by using the PolyWorks® software package, which rotates and translates the coordinate system of sphere center points from repeat surveys to that of the baseline survey. Potential errors associated with sequential survey aligning arise from (1) minor misalignments in the baseline and repeat surveys; (2) variability in repositioning the alignment spheres on the monuments; (3) variability in modeling the sphere center points for multiple surveys; and (4) monument instability.

Survey-Alignment Error

After a repeat survey was aligned to the baseline survey, a quantitative assessment of the alignment error was done using the independent set of reference spheres. Reference-sphere center points were defined from the point clouds using the PolyWorks® software package, as previously described. At each site, the reference sphere center points in the baseline and subsequent surveys (the corresponding x, y, and z center-point coordinates) were tabulated and differenced for each reference sphere. The variance of the center points along the x, y, and z axes, for each reference sphere, was used to calculate the root-mean-square error (RMSE) of the alignment.

At site 1, the alignment of the second survey (October 2015) relative to the baseline survey (December 2014) produced a RMSE of 5.6 mm and for the third survey (October 2016), the RMSE relative to the baseline survey was 10.5 mm. At site 2, the alignment of the second survey relative to the baseline survey produced a RMSE of 8.5 mm and for the third survey the RMSE relative to the baseline survey was 17.7 mm. At site 5, the alignment of the second survey relative to the baseline survey produced a RMSE of 7.1 mm and for the third survey the RMSE relative to the baseline survey was 6.7 mm.

By the time of the fourth survey (August 2017), the amount of erosion at sites 1, 2, and 5 had exceeded the anticipated erosion for the originally planned 2-year study period (2014–16). Consequently, many of the reference monuments were disturbed or completely lost to erosion, which made the quantitative assessment of alignment error impossible for the 2014–17 surveys at sites 1, 2, and 5.

At sites 1, 2, and 5, the quantitative center-point assessment produced RMSE (1-SD error) values of the alignments on the order of 5.6–17.7 mm for the 2015 and 2016 alignments relative to the baseline survey. At site 4, the 1-SD alignment error of the 2014–17 surveys was 16.1 mm.

Volumetric Calculations

Before differences in volume could be calculated, additional steps were needed to remove unwanted data points from the point clouds, to create surfaces from the land-surface points, to define a common boundary, and to define the extent of individual sedimentary units at each site within the common boundary.

Data-Point Removal

Areas of vegetation (typically less than 1.0 m^2 in area), scattered across the surface of the cliff and **colluvial slope**, were scanned during each survey (fig. 4). Small clusters of vegetation can create laser returns in front of the land surface as well as "shadows" of missing data on the land surface where vegetation blocks the laser pulse from reaching the land surface behind it. Additionally, erroneous multipath points (caused by a laser pulse bouncing off multiple objects before returning to the scanner) can be recorded. For each survey, the data were inspected individually for each sedimentary unit and any vegetation or multipath points were removed. Systematically inspecting each sedimentary unit ensured that points representing vegetation and other errant, multipath laser returns were not included in the volume calculations.

Creating Surfaces

Volume was calculated by the PolyWorks® software package, which requires a continuous 3-D surface to be generated from the land-surface points. The randomly distributed land-surface points and areas of missing data ("shadows" or areas that were not in the line-of-sight of the laser scanner) were interpolated to create a continuous surface. Using the PolyWorks® software package, a TIN (triangulated irregular network of nearest neighbor points) surface was created from the land-surface points.

Defining a Common Boundary

Prior to calculating volumes by differencing surfaces from the sequential surveys, the area of the data common to all surveys was needed. This step eliminated any effect of areal sampling bias on the calculated differences in volume resulting from a different extent of data in the surveys. From a horizontal perspective, a common data boundary for all surveys at each study site was defined. Along the outer boundaries of the mapped sedimentary units, described in the next paragraph, data for the four surveys were trimmed to match the survey with the least extent.

Mapping Sedimentary Units

Detailed field mapping of the sedimentary units was conducted at each study site. At each study site, characteristics such as sediment grain size, color, degree of cementation, and slope angle were used to differentiate sedimentary units within the exposed sequence. Using the PolyWorks® software package, the sedimentary units were mapped on the 3-D and colorized point clouds of the 2014 baseline surveys to define the areal extent of the various units at each site for volume calculations. The aligned point clouds (2014 and 2017), trimmed to a common boundary for each sedimentary unit at each study site, are publicly available (Howle, 2019).

Calculating Volumes

The PolyWorks® software package was used to calculate the volume between a user-defined fixed-reference plane and the 3-D surfaces of the sedimentary units for each survey, following methods described by Howle and others (2019). For each sedimentary unit in each survey, a surface-to-plane volume was calculated perpendicular to a fixed-reference plane. The reference planes were oriented vertically and approximately parallel to the length of the sedimentary outcrops to minimize errors in the volume calculations caused by recesses and overhanging areas of the steep outcrop surfaces. Because of the complex topography at study sites 2, 4, and 5, it was necessary to subdivide these sites into smaller areas. Site 2 was divided into southern, western, and northern areas; site 4 was divided into eastern, central, and western areas; and site 5 was divided into eastern areas 1 and 2 and western areas 1 and 2. The subdivided areas and corresponding reference planes were chosen to optimize the volumetric calculations. Using data sets for each sedimentary unit and for each time frame, the surface-to-plane volumes were calculated at an increment (discretization interval) of 1 square centimeter (cm^2). This discretization interval was integrated across the entire extent of the sedimentary units, which produced high-resolution volume measurements of each unit. The net eroded volume for each sedimentary unit was computed as the difference between the calculated volumes for the two surveys that bracket the December 2014 to August 2017 period. The calculated volumes of sediment represent the 3-D space between the initial 2014 surfaces of each sedimentary unit and the final surfaces in 2017.

Measurement of Sedimentary Unit Area

The computed net erosion volume for each sedimentary unit was combined with measurements of the corresponding surface area to estimate an erosion volume per unit area in cubic meters per square meter. So that the erosion estimates from this study can be extrapolated over a broader area of the Malakoff Diggins pit with a two-dimensional (2-D) geographic information system (GIS) application, the TLS-derived 3-D models of the sedimentary units were projected onto a horizontal plane to produce a 2-D planimetric area. Using the PolyWorks® software package, the previously described TIN surfaces for each sedimentary unit were projected onto a horizontal (x, y) plane (fig. 5). The software then calculated the 2-D planimetric area of each sedimentary unit at the centimeter-scale resolution of the TLS data.

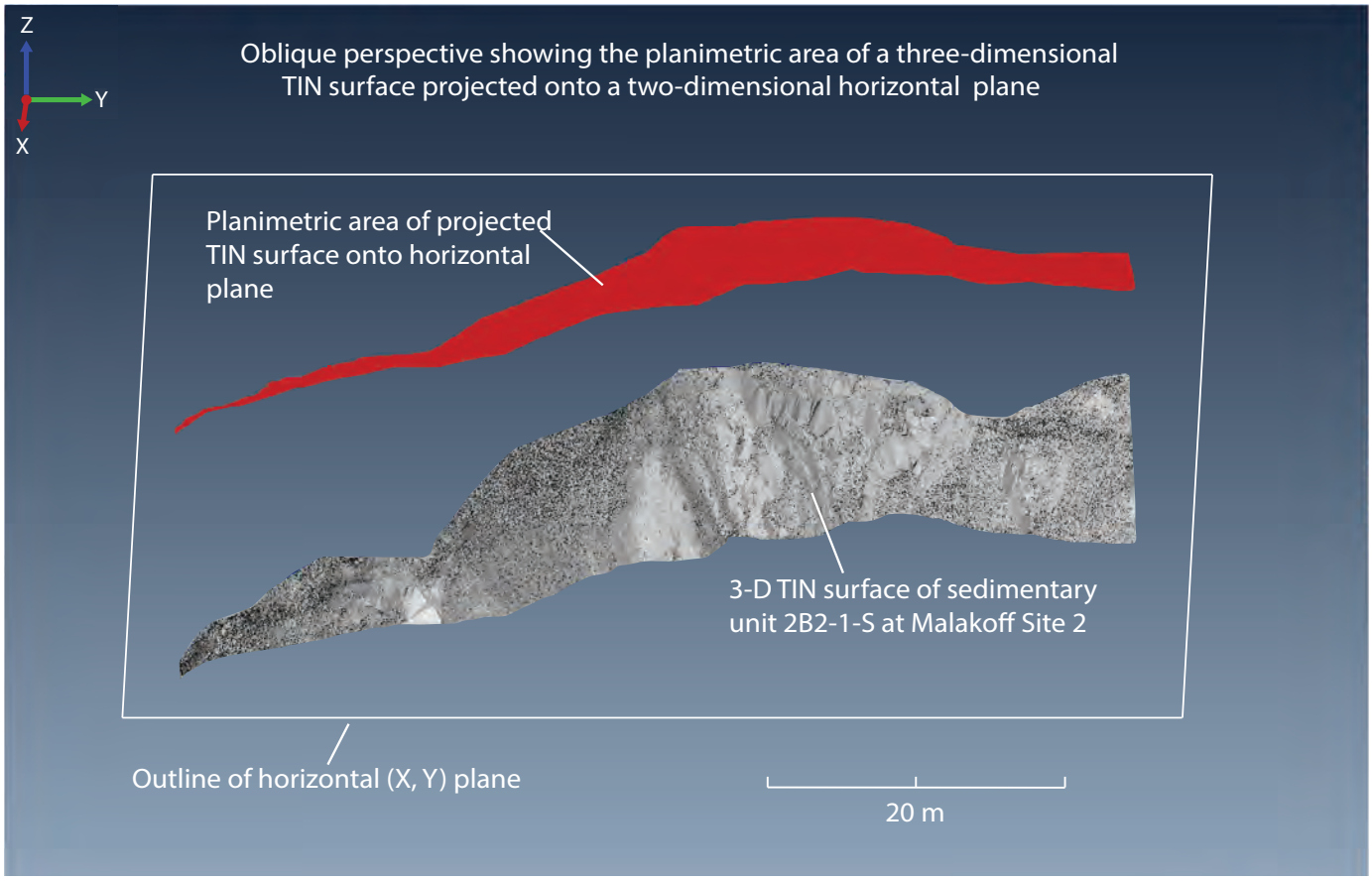

Figure 5. Oblique perspective of a three-dimensional (3-D) triangulated irregular network (TIN) surface projected onto a two-dimensional horizontal plane. Graphics displayed using PolyWorks© software.

Total Eroded Volumes

Although annual surveys were conducted at all four study sites between 2014 and 2017, only the total net erosion volumes for the December 2014 to August 2017 period are reported here. The surveys conducted during October 2015 and October 2016 were aligned and used to process the common boundary for each study site. Computation of annual net erosion volumes based on the 2015 and 2016 surveys may be done later and reported separately. The net eroded volumes for the 32-month (2.67-year) study period were computed by differencing the calculated surface-to-plane volumes for the baseline (2014) and final (2017) surveys. The calculated volumes of net eroded sediment for each sedimentary unit at study sites 1, 2, 4, and 5 represent the difference in 3-D space between the initial December 2014 surface of each sedimentary unit and the final surface in August 2017 (tables 1, 2, 3, and 4).

Table 1. Malakoff Diggings study site 1 summary of net eroded volume of sedimentary units from December 2014 to August 2017 and range of uncertainty, planimetric area of sedimentary units, erosion volume per unit area, and erosion rate.

[See figure 6 for the extent of the sedimentary units. **Abbreviations**: m^3, cubic meter; m^2, square meter; m^3/m^2, cubic meter per square meter; $m^3/m^2/yr$, cubic meter per square meter per year; ±, plus or minus; <, less than; —, not applicable]

Sedimentary unit	Net eroded volume (m^3)	Planimetric area of sedimentary unit (m^2)	Erosion volume per unit area (m^3/m^2)	Erosion rate ($m^3/m^2/yr$)
Unit 1A1	67±2	216	0.31±0.01	0.12±<0.01
Unit 1A2	171±7	391	0.44±0.02	0.16±0.01
Unit 1A3	50±4	280	0.18±0.01	0.07±<0.01
Site 1 - Totals	288±13	887	—	—
Site 1 - Average net erosion	—	—	[1]0.32±0.02	[2]0.12±0.01

[1]The average erosion volume per unit area for site 1 in cubic meters per square meter was calculated by dividing the total net eroded volume by the total planimetric area of the sedimentary units.

[2]The site 1 average erosion rate in cubic meters per square meter per year was calculated by dividing the site 1 average erosion volume per unit area in cubic meters per square meter by 2.67 years.

Table 2. Malakoff Diggings study site 2 summary of net eroded volume of sedimentary units from December 2014 to August 2017 and range of uncertainty, planimetric area of sedimentary units, erosion volume per unit area, and erosion rate.

[See appendix table 1–1 for the eroded volumes, areas of sedimentary units, values of erosion in cubic meters per square meter, and values of erosion in cubic meters per square meter per year in the southern, western, and northern areas. See figures 7–10 for the extent of the various areas and sedimentary units. **Abbreviations**: m^3, cubic meter; m^2, square meter; m^3/m^2, cubic meter per square meter; $m^3/m^2/yr$, cubic meter per square meter per year; ±, plus or minus; <, less than; —, not applicable]

Sedimentary unit	Net eroded volume (m^3)	Planimetric area of sedimentary unit (m^2)	Erosion volume per unit area (m^3/m^2)	Erosion rate ($m^3/m^2/yr$)
Unit 2A1	804±8	1,045	0.77±0.01	0.29±<0.01
Unit 2B2-1	578±23	955	0.60±0.03	0.23±0.01
Unit 2B2-2	938±28	2,142	0.44±0.01	0.16±<0.01
Unit 2C3	595±30	2,618	0.23±0.01	0.09±<0.01
Unit 2D4	326±59	1,391	0.23±0.05	0.09±0.02
Unit 2D5	42±6	451	0.09±0.01	0.03±<0.01
Site 2 - Totals	3,283±154	8,602	—	—
Site 2 - Average net erosion	—	—	[1]0.38±0.02	[2]0.14±0.01

[1]The average erosion volume per unit area for site 2 in cubic meters per square meter was calculated by dividing the total net eroded volume by the total planimetric area of the sedimentary units.

[2]The site 2 average erosion rate in cubic meters per square meter per year was calculated by dividing the site 2 average erosion volume per unit area in cubic meters per square meter by 2.67 years.

Table 3. Malakoff Diggings study site 4 summary of net eroded volume of sedimentary units from December 2014 to August 2017 and range of uncertainty, planimetric area of sedimentary units, erosion volume per unit area, and erosion rate.

[See appendix table 1–2 for the eroded volumes and area of sedimentary units in the central and eastern areas. See figures 11–14 for the extent of the various areas and sedimentary units. **Abbreviations**: m^3, cubic meter; m^2, square meter; m^3/m^2, cubic meter per square meter; $m^3/m^2/yr$, cubic meter per square meter per year; ±, plus or minus; <, less than; —, not applicable]

Sedimentary unit	Net eroded volume (m^3)	Planimetric area of sedimentary unit (m^2)	Erosion volume per unit area (m^3/m^2)	Erosion rate ($m^3/m^2/yr$)
Unit 4A1	620±6	3,377	0.18±0.01	0.07±<0.01
Unit 4A2	1,078±11	10,201	0.11±<0.01	0.04±<0.01
Unit 4A3	807±8	7,776	0.10±<0.01	0.04±<0.01
Unit 4A4	1,209±24	10,567	0.11±0.01	0.04±<0.01
Unit 4A5	2,248±45	11,979	0.19±<0.01	0.07±<0.01
Western area	2,555±51	9,095	0.28±0.01	0.10±0.01
Site 4 - Totals	8,517±145	52,995	—	—
Site 4 - Average net erosion	—	—	[1]0.16±<0.01	[2]0.06±<0.01

[1]The average erosion volume per unit area for site 4 in cubic meters per square meter was calculated by dividing the total net eroded volume by the total planimetric area of the sedimentary units.

[2]The site 4 average erosion rate in cubic meters per square meter per year was calculated by dividing the site 4 average erosion volume per unit area in cubic meters per square meter by 2.67 years.

Table 4. Malakoff Diggings study site 5 summary of net eroded volume of sedimentary units from December 2014 to August 2017 and range of uncertainty, planimetric area of sedimentary units, erosion volume per unit area, and erosion rate.

[See appendix table 1–3 for the eroded volumes and area of sedimentary units in the eastern and western areas. See figures 15–19 for the extent of the various areas and sedimentary units. **Abbreviations**: m^3, cubic meter; m^2, square meter; m^3/m^2, cubic meter per square meter; $m^3/m^2/yr$, cubic meter per square meter per year; ±, plus or minus; <, less than; —, not applicable]

Sedimentary unit	Net eroded volume (m^3)	Planimetric area of sedimentary unit (m^2)	Erosion volume per unit area (m^3/m^2)	Erosion rate ($m^3/m^2/yr$)
Unit 5A1	274±8	1,245	0.22±0.01	0.08±<0.01
Unit 5A2	168±7	393	0.43±0.02	0.16±0.01
Unit 5A3	211±2	534	0.40±<0.01	0.15±<0.01
Unit 5A4	159±2	786	0.20±<0.01	0.07±<0.01
Unit 5C5	34±3	335	0.10±0.01	0.04±<0.01
Site 5 - Totals	846±22	3,293	—	—
Site 5 - Average net erosion	—	—	[1]0.26±<0.01	[2]0.10±<0.01

[1]The average erosion volume per unit area for site 5 in cubic meters per square meter was calculated by dividing the total net eroded volume by the total planimetric area of the sedimentary units.

[2]The site 5 average erosion rate in cubic meters per square meter per year was calculated by dividing the site 5 average erosion volume per unit area in cubic meters per square meter by 2.67 years.

Estimating Volumetric Uncertainty Due to Alignment Error

The previously discussed RMSE of the sequential alignments relative to the baseline survey were used to assess potential volumetric uncertainty. As noted earlier, the reference sphere monuments at sites 1, 2, and 5 were disturbed or destroyed by the time of the final survey in August 2017. Consequently, the largest observed RMSE values at each study site (10.5 mm at site 1 in October 2016; 17.7 mm at site 2 in October 2016, and 7.1 mm at site 5 in December 2015) were used to assess potential volumetric uncertainties caused by alignment error of the 2014 and 2017 surveys. At study site 4, the RMSE alignment error of the 2014 and 2017 surveys (16.1 mm) was used for the volumetric uncertainty assessment. For all study sites the estimate was made by translating the vertical reference plane(s) along an axis perpendicular to the fixed-reference plane by plus or minus 1 RMSE value (1-SD error) and recalculating surface-to-plane volumes. The calculated volumes spanned a range equivalent to the doubled RMSE (2-SD error) for each sedimentary unit. Note that alignment errors parallel to the fixed-reference plane would not change the calculated volume and that the largest potential errors are generated from misalignments that are perpendicular to the fixed-reference plane.

Because of the relatively simple topography at site 1 (fig. 6), the range of volumetric uncertainty was calculated for each sedimentary unit in its entirety. However, at sites 2, 4, and 5 where the topography was more complex, and the sites were subdivided, the range of volumetric uncertainty for each sedimentary unit was calculated for the subdivided area with the largest planimetric area (appendix tables 1–1, 1–2, and 1–3). The calculated ±1-SD volumetric errors for the subdivided area with the largest planimetric area were used to estimate a percent volume uncertainty for the full extent of the various sedimentary units at sites 2, 4, and 5 (tables 2, 3, and 4). At these sites, the percent volume uncertainty for each sedimentary unit (table 5) was multiplied by the corresponding total net eroded volume of the subdivided units (tables 2, 3, and 4) to estimate the volumetric uncertainty of each sedimentary unit due to potential alignment error.

Visualization of Changes

Two-dimensional change plots allow for the visualization of where and how much the land surface changed at each study site and each sedimentary unit. These graphics facilitate the interpretation of the erosional processes responsible for the observed changes and provide a basis for determining where mitigation measures, if deemed necessary, would be most effective. Color-coded, 2-D change plots were created in PolyWorks® by symbolizing the horizontal distance between the December 2014 and August 2017 scanned surfaces.

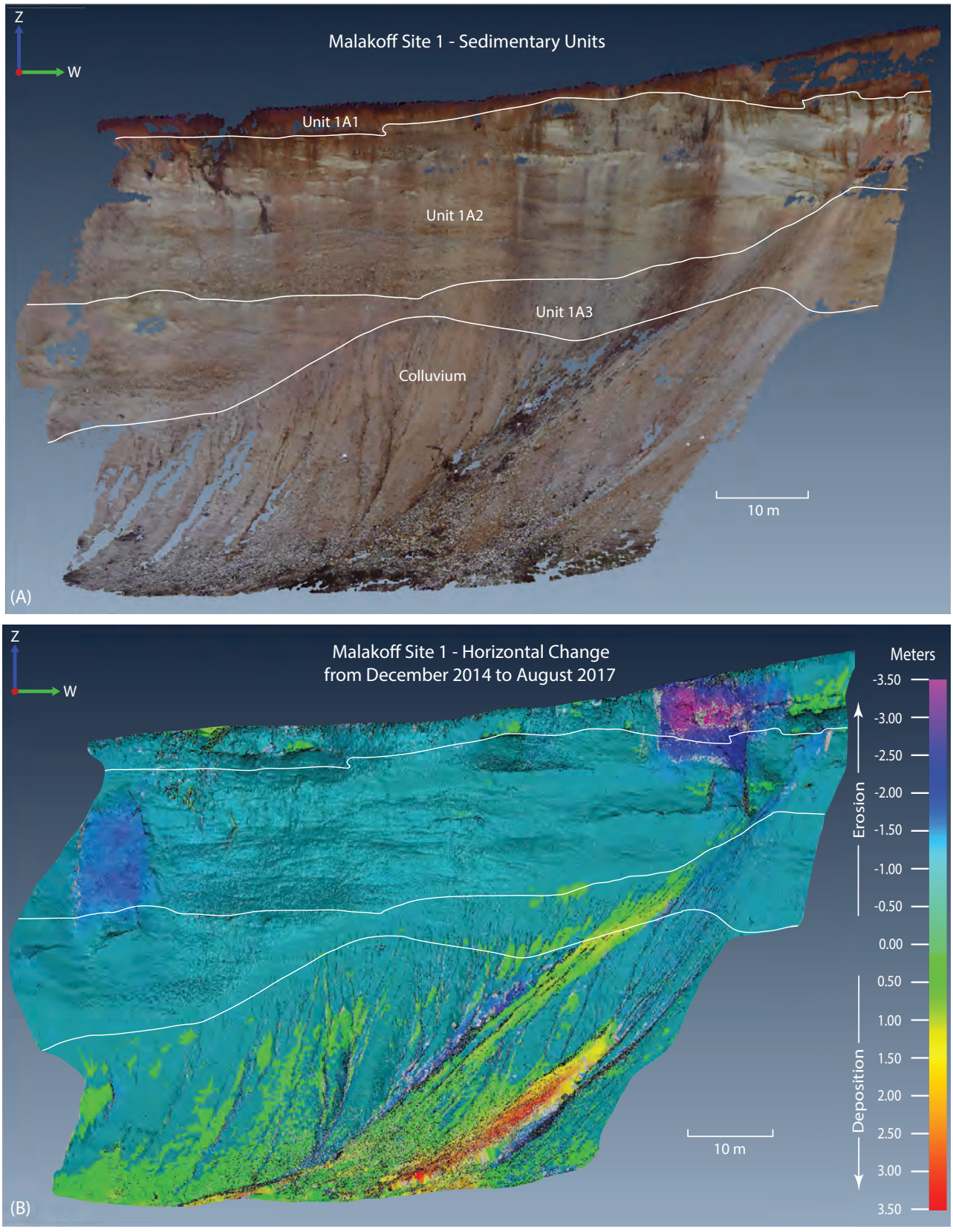

Figure 6. Malakoff Diggins study site 1. View to the south. *A*, horizontal perspective of colorized point cloud and extent of mapped sedimentary units, imagery from December 2014; and *B*, horizontal perspective of horizontal change from December 2014 to August 2017. Graphics displayed using PolyWorks© software.

Table 5. Root-mean-square error (RMSE) due to potential alignment errors in percent of net eroded volume for sedimentary units at Malakoff Diggins study sites 1, 2, 4, and 5 and average RMSE of each study site.

[See figures 6, 7, 13, 14, and 15 for extent of the various sedimentary units.]

Sedimentary unit	Volumetric RMSE, in percent of net eroded volume
1A1	3
1A2	4
1A3	8
Site 1 average	5
2A1	1
2B2-1	4
2B2-2	3
2C3	5
2D4	18
2D5	14
Site 2 average	8
4A1	1
4A2	1
4A3	1
4A4	2
4A5	2
Western area	2
Site 4 average	2
5A1	3
5A2	4
5A3	1
5A4	1
5C5	10
Site 5 average	4

Site 1

Site 1, in the southwest corner of the Malakoff Diggins mine pit (fig. 2), is a north-facing alcove, approximately 120 m wide with a planimetric area of 887 m^2 (table 1), where three sedimentary units form a 30- to 50-m-high cliff (fig. 6*A*). Across all three units, persistent erosional processes such as **dry ravel**, periodic sheet wash, and frost heave caused generally uniform horizontal erosion (retreat) ranging from about 1 to 1.5 m between December 2014 and August 2017. On the western side of unit 1A1 is a pronounced area of erosion ranging from about 2 to 3.5 m of retreat (blue to pink area in fig. 6*B*) where a block-fall failure of well-indurated sediment detached from the near-vertical cliff face and deposited a swath of coarse blocky debris on the colluvial slope below (yellow to red areas in fig. 6*B*). Similarly, on the eastern side of unit 1A2 is an area of erosion, approximately 1.5–2 m deep (light blue to blue area), which is bounded by vertically oriented scarps indicating the area detached as a block or sheet of relatively uniform thickness. In figure 6, minor rilling is also evident in unit 1A3. For the period December 2014 to August 2017, net erosion at study site 1 totaled 288±13 m^3 of sediment with 59 percent (171 m^3) coming from unit 1A2 (table 1). Dividing this total net erosion volume by the total planimetric area (887 m^2) yields an average erosion volume per unit area of 0.32±0.02 m^3/m^2 between December 2014 and August 2017. When computed on an annual basis, the surveyed area at site 1 yields an average erosion rate of 0.12±0.01 $m^3/m^2/yr$ (table 1).

Site 2

Site 2, on the western margin of Malakoff Diggins mine pit (fig. 2), is an approximately 100-m-wide amphitheater with about 40 m of vertical relief (fig. 7) and a planimetric area of about 8,600 m^2 (table 2). For volume calculations, the variability in aspect (slope direction) required that the study site be subdivided into a southern area (facing northeast), a western area (facing southeast), and a northern area (facing south). The two boundaries between the three areas coincide with deep erosional gullies (fig. 7). The three areas drain into a deeply incised southeast-trending ravine. Six distinct sedimentary units are exposed at site 2: units 2A1, 2B2-1, 2B2-2, 2C3, 2D4, and 2D5. The stratigraphically lowest unit (2D5) is exposed only in the northern area, forming a wall along the southeast-trending ravine. The sedimentary units in the southern area have distinct changes in slope angle, with units 2B2-2-S and 2D4-S forming steeper ‘cliff’ areas (fig. 8*A*) and the other units forming lower-angle slopes. The exposures of the units in the western and northern areas are generally steeper with less distinct changes in slope from one unit to another.

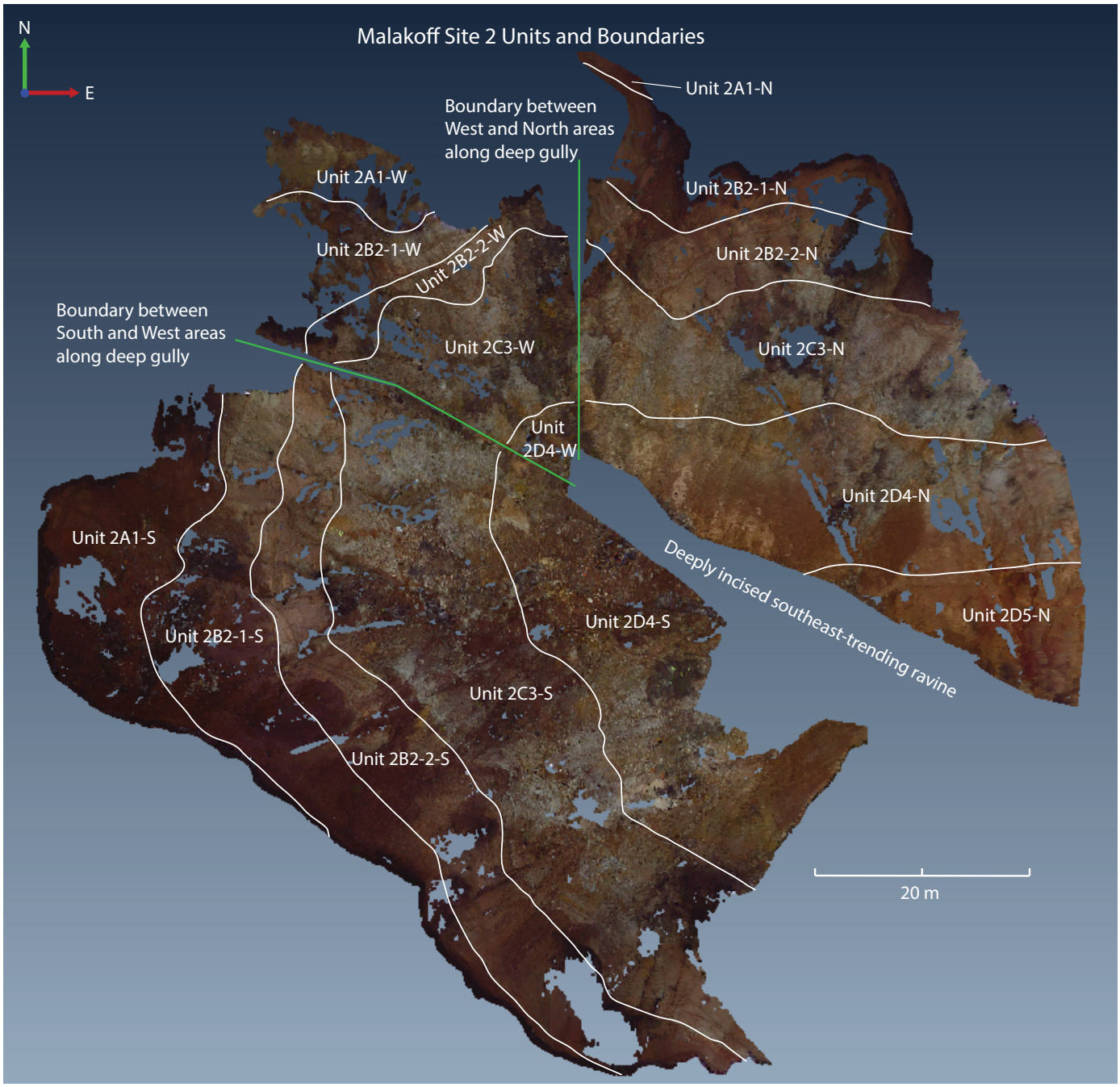

Figure 7. Planimetric extent of sedimentary units and boundaries between the southern, western, and northern areas at Malakoff Diggins study site 2. Imagery is the colorized point cloud from December 2014. Graphics displayed using PolyWorks© software.

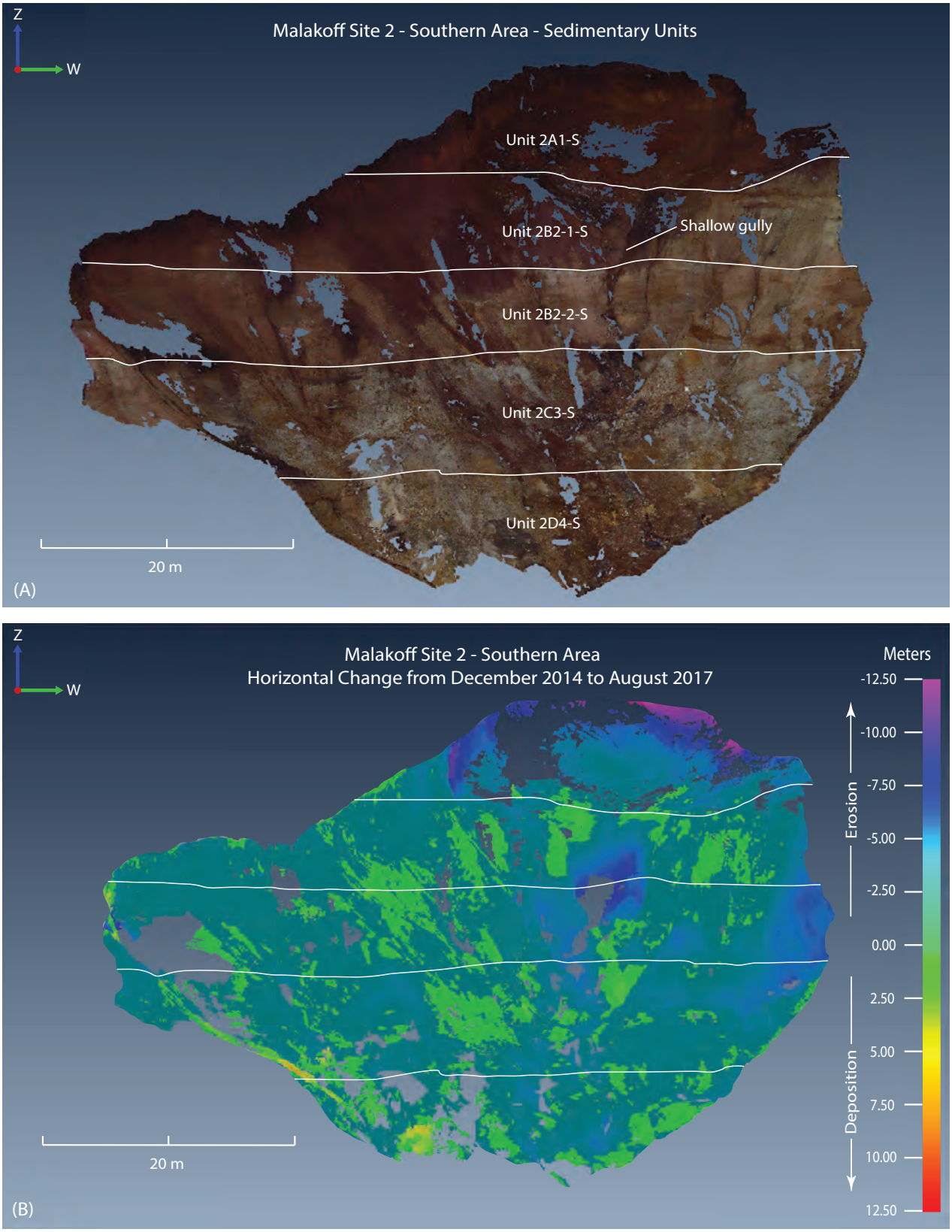

Figure 8. Southern area at Malakoff Diggins study site 2. View to the south. *A*, horizontal perspective of colorized point cloud and extent of mapped sedimentary units, imagery from December 2014; and *B*, horizontal perspective of horizontal change from December 2014 to August 2017. Background colors (shades of gray) represent missing or sparse lidar data. Graphics displayed using PolyWorks© software.

Site 2—Southern Area

In the southern area of study site 2, the most susceptible sedimentary unit to erosion was unit 2A1-S (fig. 8). During the December 2014 to August 2017 period, this unit failed twice (winters of 2015–16 and 2016–17) in rotational landslides. The rotational motion of the landslides was evidenced by trees, originally upright and above the steep 2A1-S outcrop (a former landslide head scarp), fallen on the ground and oriented in an upslope direction above the contact between units 2A1-S and 2B2-1-S. These episodic landslide events caused horizontal retreat ranging from about 7 to 12.5 m (blue to pink areas in fig. 8*B*). In units 2B2-1-S and 2B2-2-S, below the central part of unit 2A1-S, was a localized area of erosion ranging from about 5 to 7.5 m (light blue to dark blue in fig. 8*B*) that likely was caused by scouring as the landslide(s) coalesced into a shallow gully (fig. 8*A*). Along the western margin of the southern area, primarily in unit 2B2-2-S, erosion of about 6–7 m (blue to dark blue area in fig. 8*B*) occurred adjacent to the gully that divides the southern and western areas, likely caused by water-saturated debris flows concentrated in the gully. Below unit 2A1-S, there was widespread horizontal retreat (erosion), generally less than 2.5 m (green to light blue areas in fig. 8*B*), while less extensive areas had localized deposition of up to approximately 2.5 m (green to dark green areas). In the lowest units (2C3-S and 2D4-S), localized deposition exceeding 5 m was evident (yellow to orange areas in fig. 8*B*). Despite the areas of deposition, all units in the southern area had net erosion. The total 2014–17 net erosion in the southern area was 1,554 m^3, with 46 percent of that volume (716 m^3) originating from the upper 2A1-S unit. The fact that 46 percent of the total volume originated from the upper 2A1-S unit indicates that horizontal retreat of the pit rim is the dominant erosional process at this site. See appendix table 1–1 for details of erosion volumes in the southern, western, and northern areas of site 2.

Site 2—Western Area

In the western area of site 2, the greatest horizontal retreat of about 4.5 m was in unit 2B2-1-W (fig. 9*A*), along the southern margin near the previously mentioned gully separating the southern and western areas (pink areas in fig. 9*B*). Here again, the deep incision was presumably caused by water-saturated debris flows concentrated in the gully between the southern and western areas. Another area of approximately 3–4.5 m of horizontal retreat occurred in the middle of the western area (in units 2B2-1-W and 2B2-2-W) along narrow and vertically oriented gullies (fig. 9). Sheet wash from above the gullies apparently coalesced and concentrated erosion in the gullies (purple to pink area in the center of fig. 9*B*). Superimposed on this area of erosion are angular areas (yellow to orange patches in fig. 9*B*) that represent the deposition of coherent blocks of sediment possibly derived from unit 2A1-W or farther upslope. All units in the western area except the lowest (2D4-W) had net erosion during the December 2014 to August 2017 period. The total 2014–17 net erosion in the western area was 610 m^3, with 39 percent of that volume (239 m^3) originating from unit 2B2-2-W and 34 percent (210 m^3) originating from unit 2B2-1-W (appendix table 1–1).

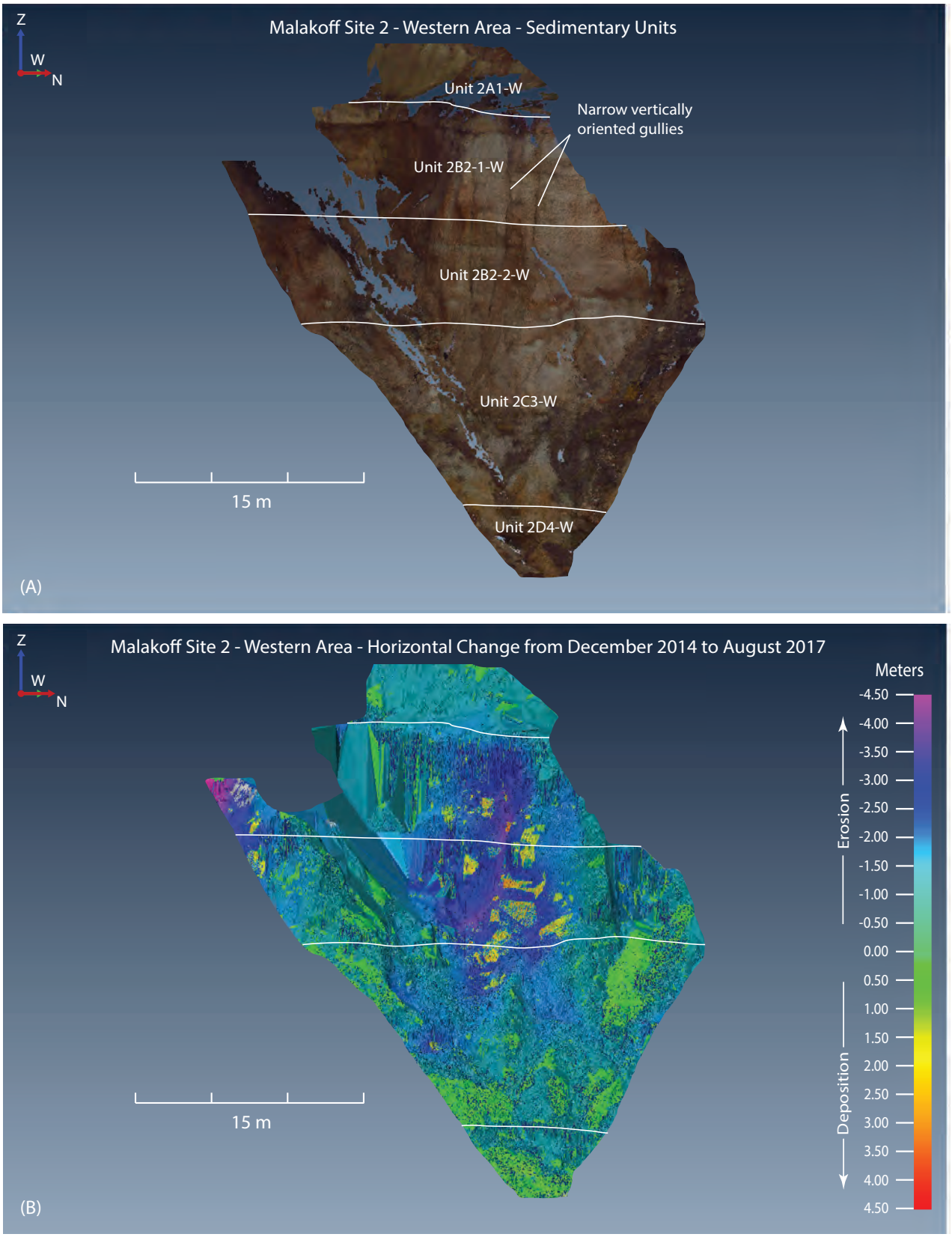

Figure 9. Western area at Malakoff Diggins study site 2. View to the south-southwest. *A*, horizontal perspective of colorized point cloud and extent of mapped sedimentary units, imagery from December 2014; and *B*, horizontal perspective of horizontal change from December 2014 to August 2017. Background colors (shades of gray) represent missing or sparse lidar data. Graphics displayed using PolyWorks© software.

Site 2—Northern Area

In the northern area of site 2 (fig. 10*A*), the greatest amount of horizontal retreat, ranging from 6 to 10 m (blue to pink area in fig. 10*B*), occurred in units 2B2-1-N and 2B2-2-N along the gully that divides the western and northern areas. All units in the northern area had localized horizontal retreat of at least 3–4 m (light blue areas). Despite localized areas of deposition varying from approximately 1 to 3 m (light green to light yellow areas in fig. 10*B*), all units had net erosion during the study period. The total 2014–17 net erosion in the northern area was 1,119 m^3, with 30 percent of that volume (341 m^3) originating from unit 2B2-2-N and 22 percent (243 m^3) originating from unit 2D4-N (appendix table 1–1).

Site 2—Combined Areas

At study site 2, the combined net erosion for all six units in the southern, western, and northern areas totals 3,283±154 m^3 (table 2). The ranking of sedimentary units at study site 2 in terms of the net volume of sediment eroded during the December 2014 to August 2017 period is as follows: unit 2B2-2 (939±28 m^3), unit 2A1 (804±8 m^3), unit 2C3 (595±30 m^3), unit 2B2-1 (578±23 m^3), unit 2D4 (325±59 m^3) and unit 2D5 (42±6 m^3; fig. 7 and table 2). Dividing the total net erosion volume (3,283±154 m^3) by the total planimetric area (8,602 m^2) yields an average erosion volume per unit area of 0.38±0.02 m^3/m^2 between December 2014 and August 2017. When computed on an annual basis, the surveyed area at site 2 yields an average erosion rate of 0.14±0.01 $m^3/m^2/yr$ (table 2). The area-normalized erosion rate in cubic meters per square meter per year decreased from top to bottom through the stratigraphic sequence (table 2).

Site 4

Site 4, located in the northeast corner of the Malakoff Diggins mine pit (fig. 2), is a 500-m-wide area composed of three separate cliff areas (western, central, and eastern). During reconnaissance visits prior to the surveys, it was recognized that the cliff areas at study site 4 delivered large volumes of sediment to the pit floor and that episodic landslides were most likely a dominant mechanism of the erosion there (fig. 3). Because of its relatively large area, the hypothesized erosion mechanism (landslides), and difficult access, a long-range laser scanner was identified as the most efficient TLS equipment for imaging the three areas (fig. 11). Mapping of the sedimentary units at site 4 was done at the eastern cliff area. The five sedimentary units exposed in the eastern area were readily correlated to the central cliff area but not to the western outcrop. Consequently, the measured erosion of the sedimentary sequence in the western area was not differentiated.

Site 4—Western Area

The western area of site 4 is approximately 100 m wide and 40 m high (fig. 12) with a planimetric area of 9,095 m^2 (table 3). Across the top of the western area, there was typically about 2–3 m of horizontal retreat (light blue areas in fig. 12*B*) during the December 2014 to August 2017 period. Below these areas of erosion was widespread deposition in the range of 0.5–1.5 m (green areas). In the middle of the western area, along the upper boundary, is a 10-m-wide zone of deposition less than or equal to approximately 1 m. This area indicates that sediment was transported from the slope above the pit rim in the western area (fig. 11). In the upper right part of the western area, at approximately three-quarters of the total height, is an area of iron-oxide staining below an over-hanging section of the cliff (fig. 12*A*). This area coincides with approximately 4 m of horizontal retreat (right-slanting area of dark blue in fig. 12*B*). Large iron-oxide-stained blocks of sediment are visible on the colluvial slope below (fig. 12*A*), indicating the source area was from the upper right part of the cliff beneath the over-hanging cliff. This coarse, blocky deposit is indicative of a block-fall failure. The coarse deposit of iron-oxide-stained blocks rests on a larger apron of colluvial debris (colluvial footslope), that lies below a deep and wide gully bounding the eastern side of the cliff. The entire surface of colluvial foot slope had 4–5 m of horizontal retreat (dark blue area in the lower right of fig. 12*B*), indicating that a large scouring event emanated from the deep and wide gully. This scouring event might also have undermined the eastern base of the cliff, where 6–7 m of horizontal change (erosion) occurred (purple to pink area in fig. 12*B*). The total 2014–17 net erosion in the western area of site 4 was 2,555±51 m^3 (table 3).

Site 4—Central Area

The central area of study site 4 is approximately 60 m wide and 20 m high (fig. 13) with a planimetric area of 1,110 m^2 (appendix table 1–2). Like the western area, erosion and deposition were measured across the upper part of the outcrop (unit 4A1-C), indicating that sediment was transported downslope from above the pit rim. The central area had widespread deposition generally less than or equal to 1 m (areas of green in fig. 13*B*), and sedimentary units 4A1-C, 4A2-C, 4A3-C, and 4A4-C had net erosion during the study period (appendix table 1–2), totaling 81 m^3. The greatest horizontal retreat of about 4 m (purple area in lower left of fig. 13*B*) was in the lowest unit (4A5-C), where 82 m^3 of erosion occurred. This volume accounted for 51 percent of the total net eroded volume (163 m^3) at the central area of site 4 during the 2014–17 period (appendix table 1–2).

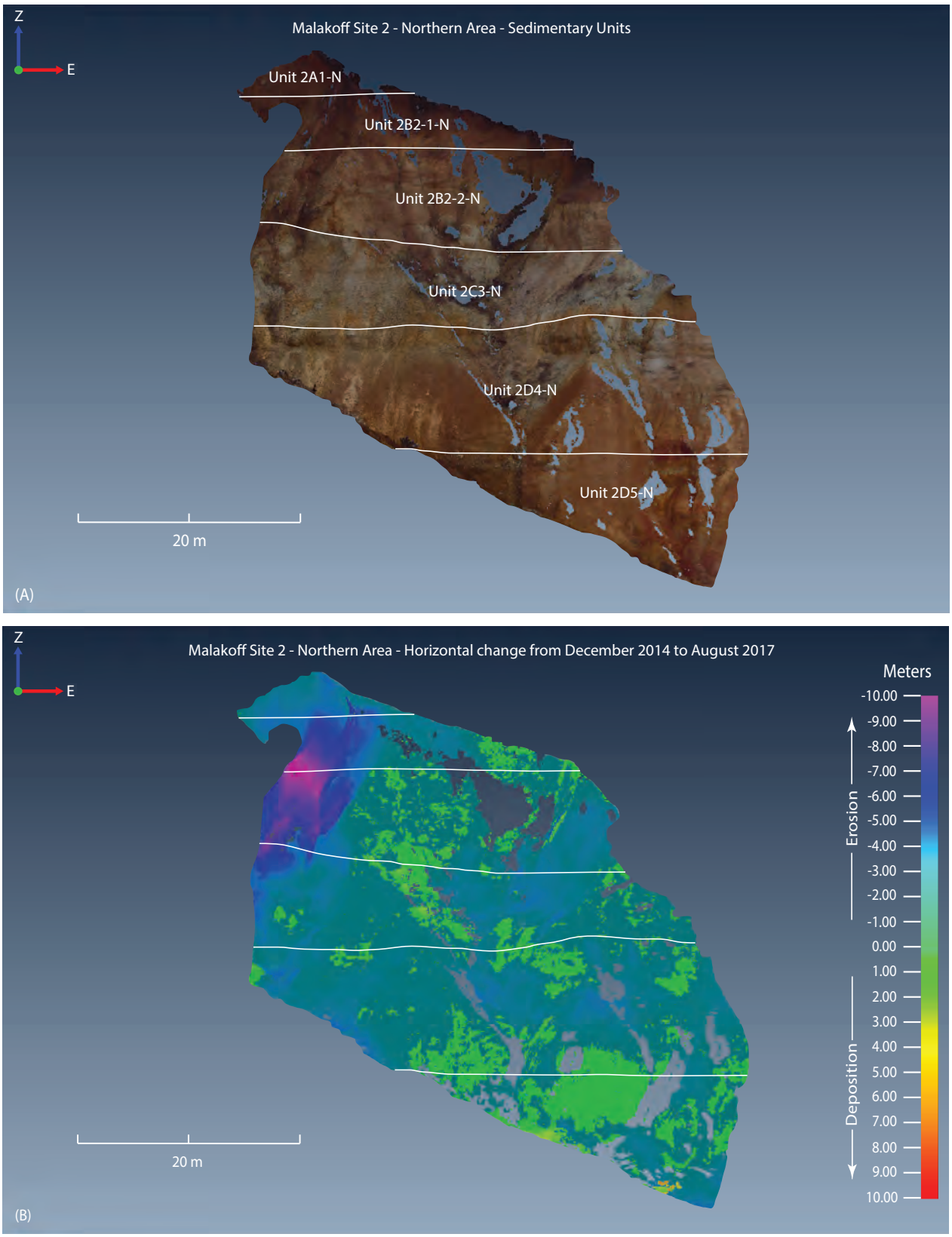

Figure 10. Northern area at Malakoff Diggins study site 2. View to the north. *A*, horizontal perspective of colorized point cloud and extent of mapped sedimentary units, imagery from December 2014; and *B*, horizontal perspective of horizontal change from December 2014 to August 2017. Background colors (shades of gray) represent missing or sparse lidar data. Graphics displayed using PolyWorks© software.

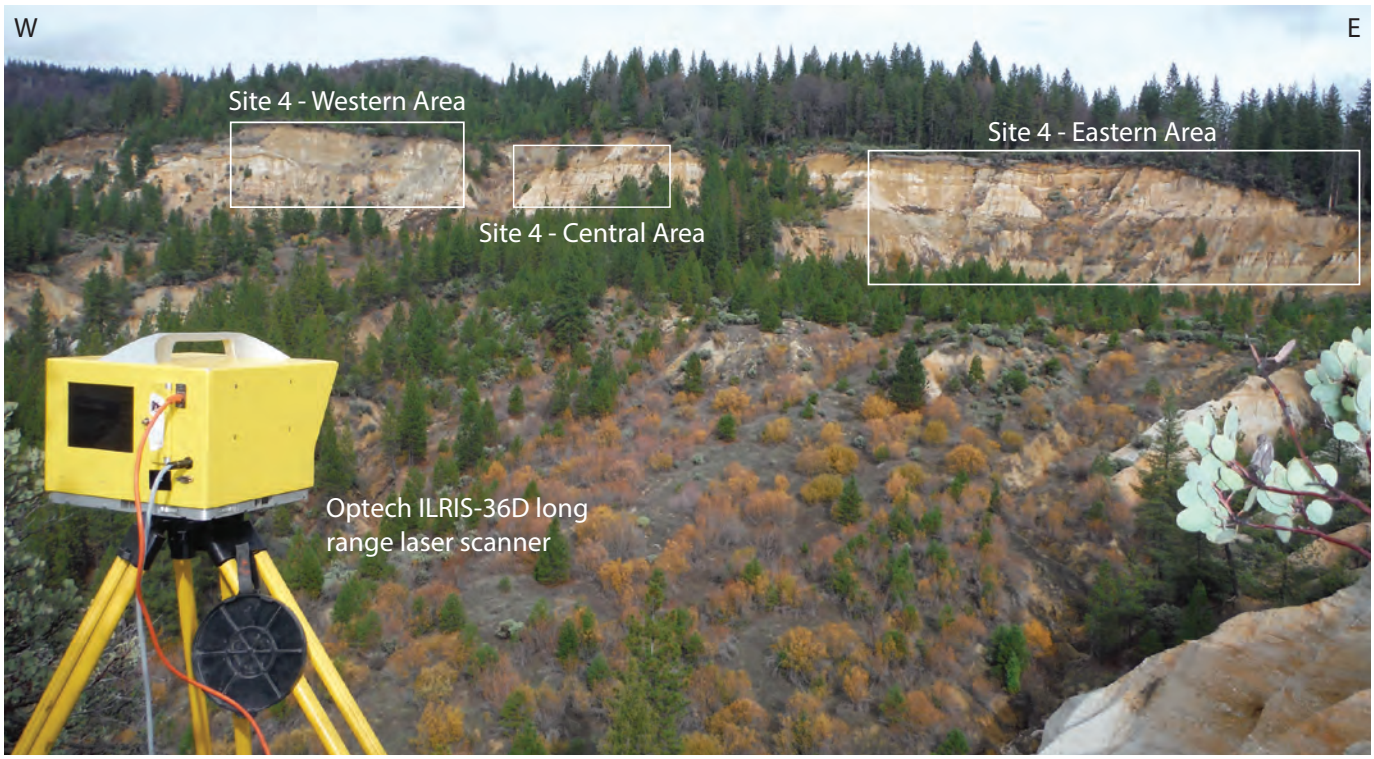

Figure 11. Western, central, and eastern areas of Malakoff Diggins study site 4 and long-range Optech ILRIS laser scanner. Photograph taken December 10, 2014, by A.J. Ward, U.S. Geological Survey.

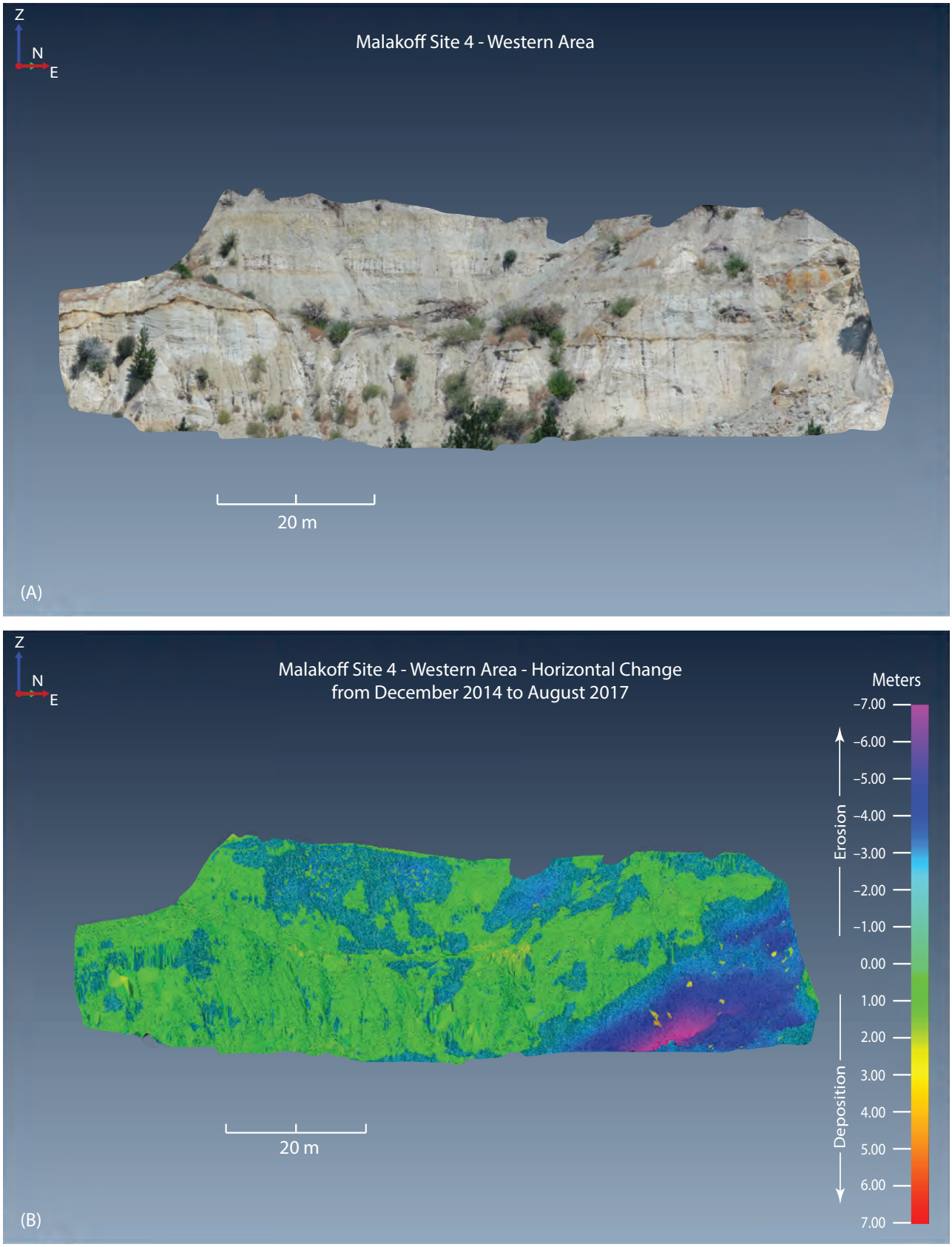

Figure 12. Western area of Malakoff Diggins study site 4. View to the north-northwest. *A*, color photograph showing the extent of the undifferentiated sedimentary units in the western area, image taken October 22, 2015; and *B*, horizontal perspective of horizontal change from December 2014 to August 2017. Graphics displayed using PolyWorks© software.

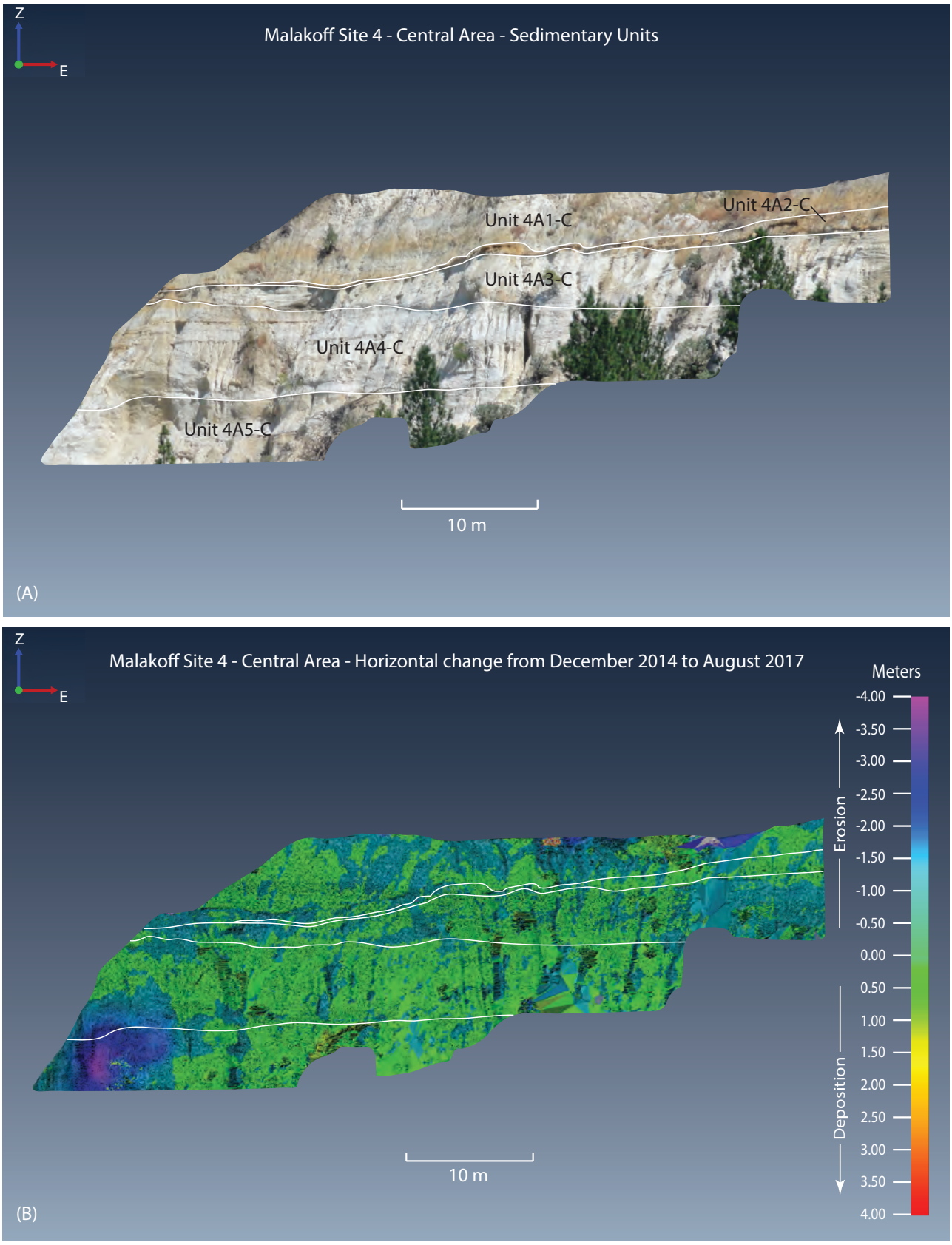

Figure 13. Central area of Malakoff Diggins study site 4. View to the north. *A*, color photograph showing the extent of the central area and sedimentary units, image taken October 22, 2015; and *B*, horizontal perspective of horizontal change from December 2014 to August 2017. Graphics displayed using PolyWorks© software.

Site 4—Eastern Area

The eastern area of study site 4 is approximately 160 m wide and 45 m high (fig. 14) with a planimetric area of 41,962 m^2 (appendix table 1–2). At the eastern area of study site 4, the largest area of horizontal retreat occurred in units 4A1-E and 4A2-E just below the top of the cliff near the western side. In this area, the horizontal retreat was about 7–9 m (purple to pink areas in fig. 14*B*). Based on field observations, this steep landslide head scarp collapsed sometime during the winter of 2016–17. Previously, incipient head-scarp cracks had been observed in the grassy slope (fig. 14*C*) as early as October 2014. All sedimentary units in the eastern area of study site 4 had localized areas where approximately 7–9 m of horizontal retreat occurred (small purple to pink areas in fig. 14*B*). The next largest areas of horizontal retreat occurred along the western and eastern margins of units 4A2-E and 4A3-E. In these areas, the pit wall retreated horizontally between 5 and 6 m (dark blue areas in fig. 14*B*) from December 2014 to August 2017. In other steep areas, typically where vegetation was not present (fig. 14*A*), horizontal retreat was on the order of 3–4 m (areas of light blue in fig. 14*B*). Deposition ranging from 1 to 2 m (green to yellow areas in fig. 14*B*) occurred on gentler slopes and, in many areas, coincided with vegetation, which could have stabilized the downslope movement of sediment.

All sedimentary units in the eastern area of study site 4 had net erosion, which totaled 5,799 m^3 for the 2014–17 period (appendix table 1–2). Of that total, 37 percent (2,166 m^3) came from unit 4A5-E, followed by units 4A4-E (21 percent or 1,202 m^3) and 4A2-E (18 percent or 1,068 m^3; appendix table 1–2).

Site 4—Combined Areas

At study site 4, the combined net erosion for the western, central, and eastern areas totaled 8,517±145 m^3 (table 3). The ranking of sedimentary units in the central and eastern areas of site 4 with regard to the net volume of sediment eroded during the December 2014 to August 2017 period is as follows: unit 4A5 (2,248±45 m^3), unit 4A4 (1,209±24 m^3), unit 4A2 (1,078±11 m^3), unit 4A3 (807±8 m^3), and unit 4A1 (620±6 m^3; figs. 13, 14, and table 3). Dividing the total net erosion volume (8,517±145 m^3) by the total planimetric area (52,995 m^2) yielded an average erosion volume per unit area of 0.16±<0.01 m^3/m^2. When computed as an annual rate, the three areas at site 4 produced an erosion rate of 0.06±<0.01 $m^3/m^2/yr$ (table 3). The relatively low rate of erosion at site 4 might be because of a lower frequency of landslide failures compared with more persistent erosion mechanisms at the other study sites.

Site 5

Site 5, located in the southeast part of the Malakoff Diggins mine pit (fig. 2), is north-facing, approximately 100 m wide and 40 m high, and composed of two deeply dissected alcoves (eastern and western, fig. 15) with a combined planimetric area of about 3,290 m^2 (table 4). For volume calculations, the complexity of the topography required that the study site be divided into two halves (eastern and western) that were further subdivided into two sections (E1, E2 and W1, W2, fig. 15). The boundary between the east and west halves was along a narrow ridgeline, whereas the boundaries between the E1, E2 and W1, W2 sections coincide with deep, steep-walled gullies (fig. 15).

Five sedimentary units are exposed in each of the four sections (E1, E2, W1, and W2) at site 5 (figs. 16–19). At site 5, the sedimentary unit most susceptible to erosion was the uppermost (5A1) which had horizontal retreat of up to 4 m (fig. 19). This unit also produced the largest net eroded volume (274±8 m^3) during the 2014–17 period (table 4). In all four sections (E1, E2, W1, and W2), unit 5A1 had localized rotational failures (figs. 16*B*, 17*B*, 18*B*, and 19*B*) of the fine-grained and weakly consolidated sediment. The steep slopes of the stratigraphically lower units 5A2 and 5A3 had localized areas where up to 2.5 m of horizontal retreat occurred (figs. 16, 19), but in all four sections there was 0.5–1.5 m of horizontal erosion across these units (figs. 16–19). The stratigraphically lowest units 5A4 and 5C5 also had about 0.5–1.5 m of horizontal retreat over most of the outcrops; however, because these slopes were at lower angles, localized areas of deposition were measured ranging in thickness from 0.25 to approximately 1 m (figs. 16–19). The generally uniform horizontal retreat across the surfaces of the lower four units (5A2, 5A3, 5A4, and 5C5, figs. 16–19) indicate that persistent and evenly distributed erosional processes such as dry ravel, sheet wash, rilling, and frost heave were the primary erosion mechanisms.

All five sedimentary units in each section at site 5 had net erosion (appendix table 1–3) that totaled 846±22 m^3 for the December 2014 to August 2017 period (table 4). The ranking of the sedimentary units with regard to the net volume of sediment eroded during the 2014 to 2017 period is as follows: unit 5A1 (274±8 m^3), unit 5A3 (211±2 m^3), unit 5A2 (168±7 m^3), unit 5A4 (159±2 m^3), and unit 5C5 (34±3 m^3; fig. 15 and table 4). Dividing the total net eroded volume (846±22 m^3) by the total planimetric area (3,293 m^2) yielded an average erosion volume per unit area of 0.26±<0.01 m^3/m^2. Computed on an annual basis, the surveyed erosion at site 5 yielded an average erosion rate of 0.10±<0.01 $m^3/m^2/yr$ (table 4).

Combined Eroded Volume of All Study Sites

The total net eroded volume of all four study sites at Malakoff Diggins mine pit from December 2014 to August 2017 was 12,934±334 m^3, and the total planimetric area of the study sites was 65,777 m^2 (table 6). The arithmetic mean of the average erosion volume per unit area of the four study sites was 0.28+0.10/−0.12 m^3/m^2, which yielded an annual erosion rate of 0.10±0.04 $m^3/m^2/yr$ (table 6).

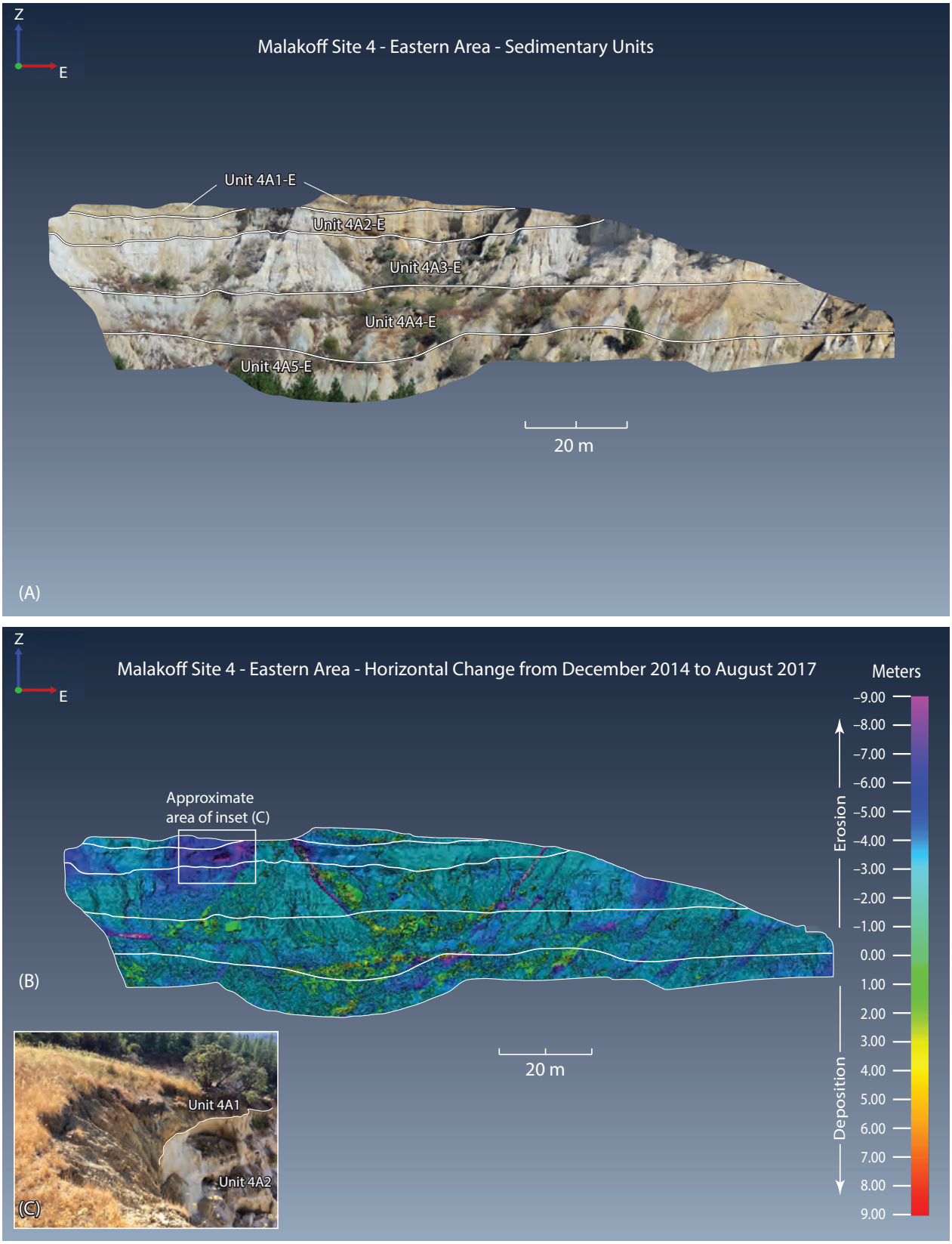

Figure 14. Eastern area of Malakoff Diggins study site 4. View to the north. *A*, color photograph showing the extent of the eastern area and sedimentary units, image taken October 22, 2015; *B*, horizontal perspective of horizontal change from December 2014 to August 2017; and *C*, inset oblique photograph showing land-slide head scarp at the eastern area, photograph taken August 24, 2017. Graphics displayed using PolyWorks© software.

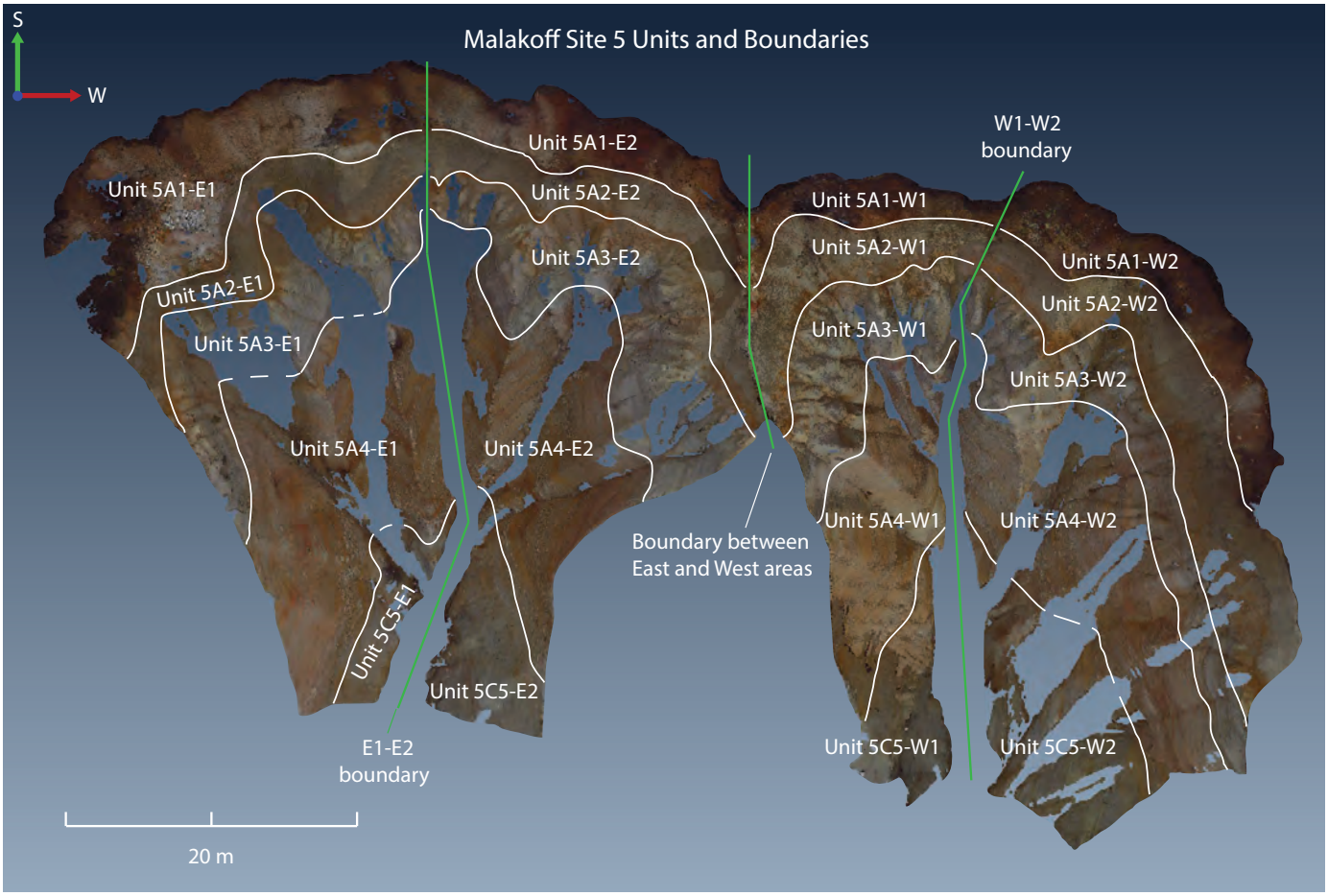

Figure 15. Planimetric extent of sedimentary units and boundaries between and within the eastern and western areas at Malakoff Diggins study site 5. Imagery is the colorized point cloud from December 2014.

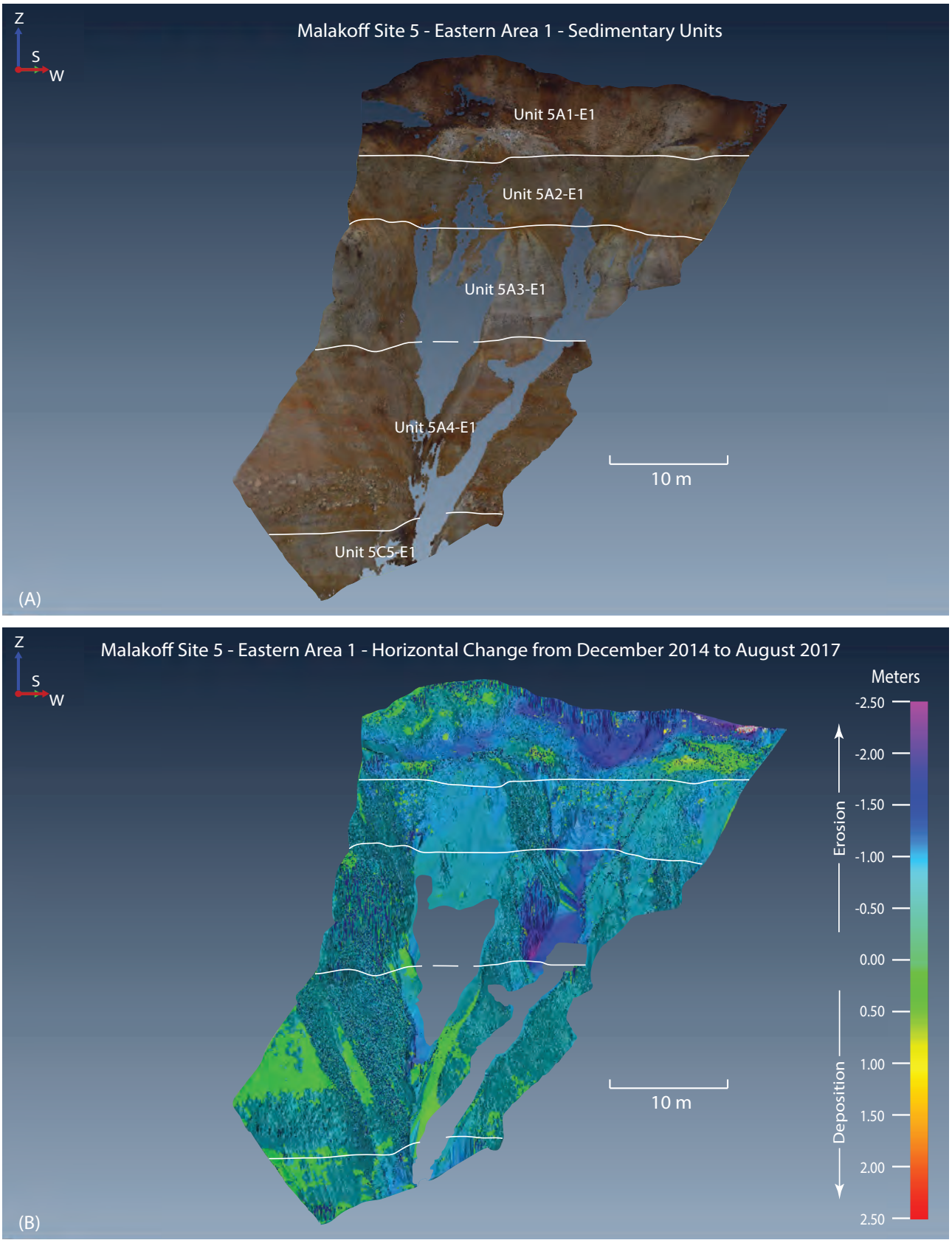

Figure 16. Eastern area 1 at Malakoff Diggins study site 5. View to the south-southeast. *A*, horizontal perspective of colorized point cloud and extent of mapped sedimentary units, imagery from December 2014; and *B*, horizontal perspective of horizontal change from December 2014 to August 2017. Graphics displayed using PolyWorks© software.

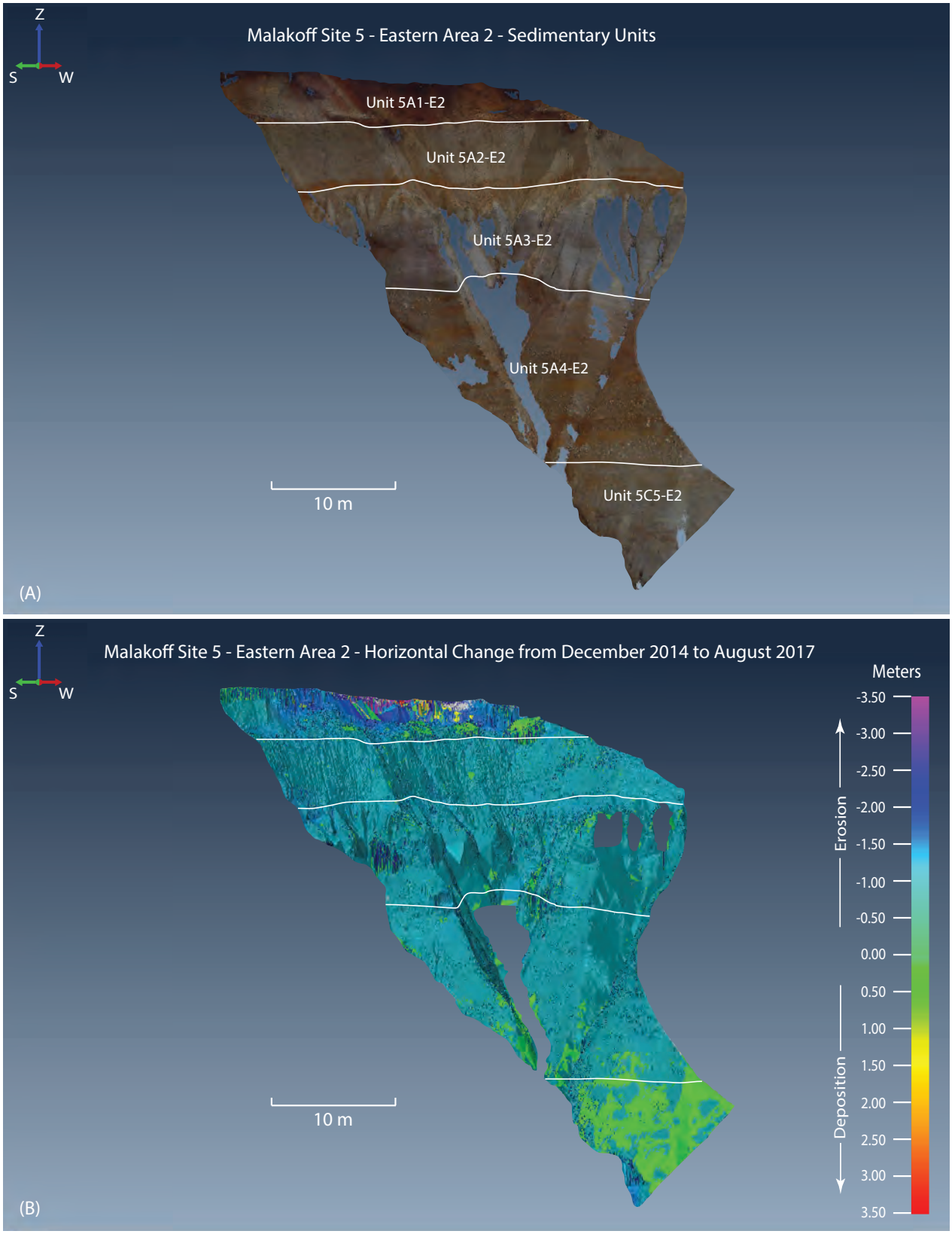

Figure 17. Eastern area 2 at Malakoff Diggins study site 5. View to the southwest. *A*, horizontal perspective of colorized point cloud and extent of mapped sedimentary units, imagery from December 2014; and *B*, horizontal perspective of horizontal change from December 2014 to August 2017. Graphics displayed using PolyWorks© software.

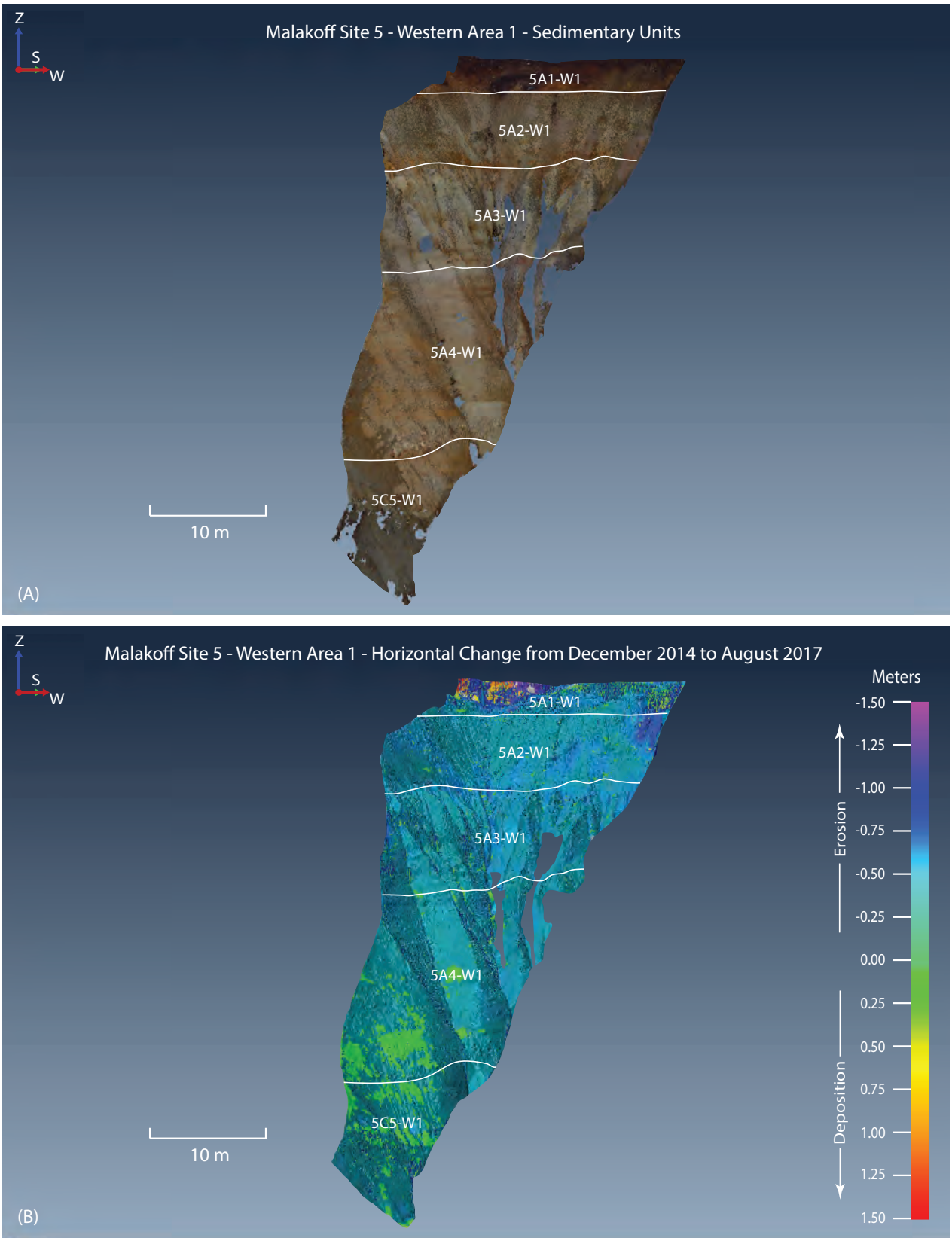

Figure 18. Western area 1 at Malakoff Diggins study site 5. View to the south-southeast. *A*, horizontal perspective of colorized point cloud and extent of mapped sedimentary units, imagery from December 2014; and *B*, horizontal perspective of horizontal change from December 2014 to August 2017. Graphics displayed using PolyWorks© software.

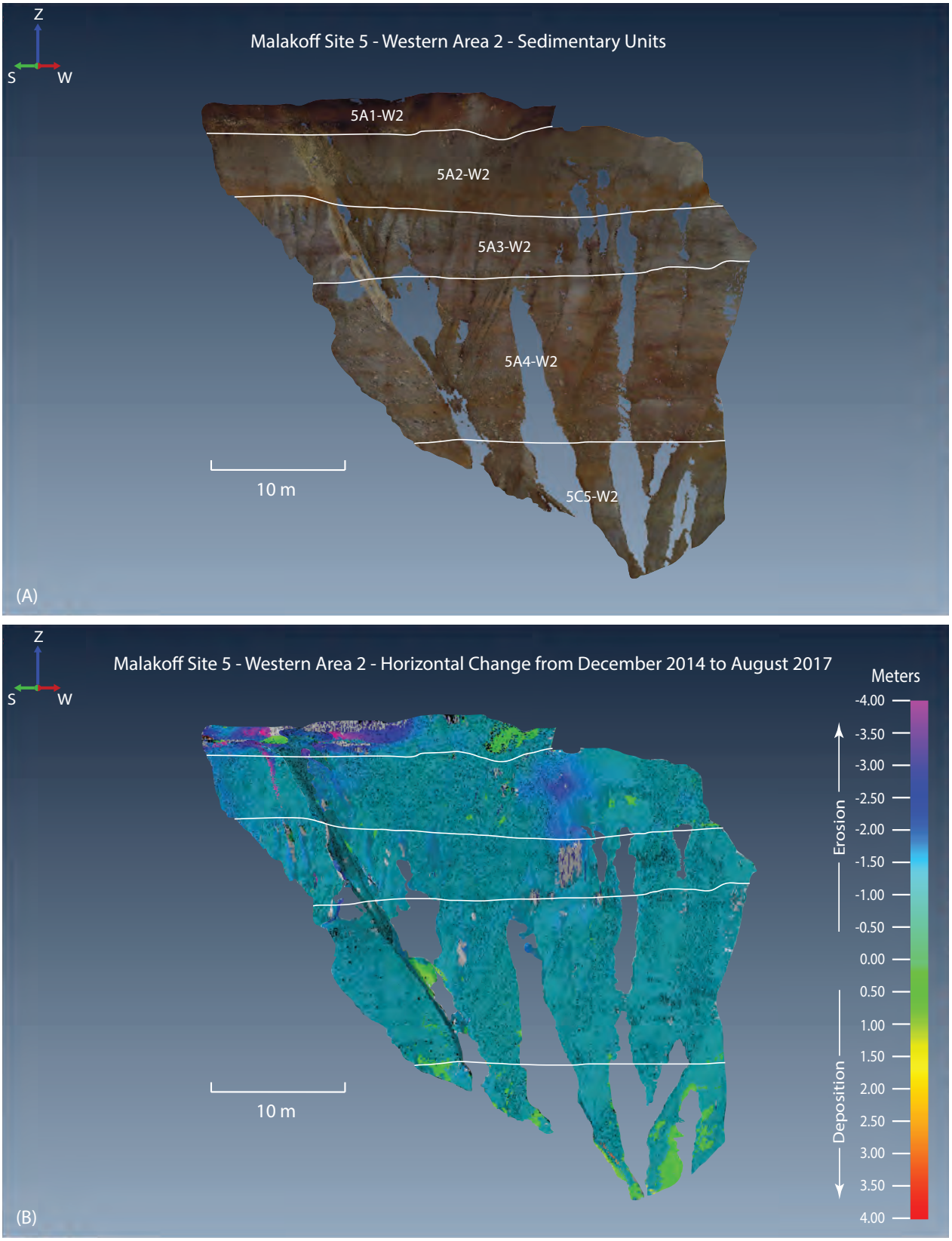

Figure 19. Western area 2 at Malakoff Diggins study site 5. View to the southwest. *A*, horizontal perspective of colorized point cloud and extent of mapped sedimentary units, imagery from December 2014; and *B*, horizontal perspective of horizontal change from December 2014 to August 2017. Graphics displayed using PolyWorks© software.

Table 6. Summary of total net eroded volume, total planimetric area of sedimentary units, average erosion volume per unit area, and average erosion rate per year for each study site from December 2014 to August 2017 at Malakoff Diggins mine pit, Nevada County, California.

[m^3, cubic meter; m^2, square meter; m^3/m^2, cubic meter per square meter; $m^3/m^2/yr$, cubic meter per square meter per year; ±, plus or minus; <, less than; —, not applicable]

Study site	Number of sedimentary units	Total net eroded volume (m^3)	Total planimetric area of sedimentary units (m^2)	Average erosion volume per unit area (m^3/m^2)	Average erosion rate ($m^3/m^2/yr$)
Site 1	3	288±13	887	0.32±0.02	0.12±0.01
Site 2	6	3,283±154	8,602	0.38±0.02	0.14±0.01
Site 4	[1]5	8,517±145	52,995	0.16±<0.01	0.06±<0.01
Site 5	5	846±22	3,293	0.26±<0.01	0.10±<0.01
Total of all study sites	19	12,934±334	65,777	—	—
Average net erosion for all study sites	—	—	—	[2]0.28+0.10/–0.12	[3]0.10±0.04

[1]At site 4, the total net eroded volume and the total planimetric area of sedimentary units includes the undifferentiated western area.

[2]The average erosion per unit area in cubic meters per square meter for all study sites was calculated by averaging the erosion per unit area in cubic meters per square meter for each study site (0.32, 0.38, 0.16 and 0.26) and the plus or minus uncertainty (+0.10/–0.12) represents the variance relative to the average value.

[3]The average erosion rate in cubic meters per square meter per year for all study sites was calculated by averaging the erosion rate in cubic meters per square meter per year for each study site (0.12, 0.14, 0.06 and 0.10) and the plus or minus uncertainty (±0.04) represents the variance relative to the average value.

Summary

The abandoned hydraulic mine pit at Malakoff Diggins near Grass Valley, California, can produce large volumes of sediment during rainfall-runoff events. The sediment-laden water discharged from the pit through the Hiller Tunnel is a major source of heavy metals to Humbug Creek and the South Yuba River. To develop a comprehensive sediment budget for the Malakoff Diggins mine pit that will help identify sources of sediment and metals within the pit that can become entrained as suspended sediment in runoff discharged from the pit into Humbug Creek, the U.S. Geological Survey (USGS), working in cooperation with the California Department of Water Resources, the California Department of Parks and Recreation, and the Nevada Irrigation District, used terrestrial laser scanning (TLS) technology to quantify eroded volumes and erosion rates of sedimentary units exposed in the pit walls. The results for eroded volumes and rates reported here are part one of a three-part study. Results from remaining parts of the investigation will use descriptions of mineralogy and chemical constituents of fine-grained sediment to assess sources of sediment and metals within the pit that can become entrained and transported beyond the Malakoff Diggins mine pit. Results from parts 2 and 3 are published separately (Ward and others, 2019), as will the final assessments.

The purpose of this report is to document the methods used and the net volume of eroded sediment, as well as the rate of erosion, for 19 sedimentary units at 4 study sites (1, 2, 4, and 5) in the Malakoff Diggins mine pit from December 2014 to August 2017. Sequential TLS surveys were an effective method to quantify volumetric changes of complex, eroding surfaces that could not have been mapped with traditional surveying techniques. The non-destructive scanning of the outcrops and the centimeter-scale resolution of the resulting point clouds allowed for a spatially detailed assessment of change across the various sedimentary units.

In this study, four sequential TLS surveys were completed; however, only the initial baseline survey in December 2014 and the final survey in August 2017 were analyzed quantitatively. Each survey at each site was composed of multiple TLS scans collected from different vantages which were combined into a composite three-dimensional (3-D) point cloud of the study site. The sequential surveys were co-registered or ‘aligned’ into a common 3-D reference frame so that volumetric comparisons between surveys could be made. For volume calculations, detailed field mapping of the sedimentary units at each study site were transferred to the 3-D and colorized point clouds of the 2014 surveys to define the extent of the sedimentary units at each site. For the baseline and final surveys at each study site and for each sedimentary unit, a volume was computed between a fixed-reference plane and the scanned land surface. Volumetric changes were computed as the difference between the calculated volumes for the two surveys that bracket the December 2014 to August 2017 period. The calculated volumes of sediment represent the 3-D space between the initial 2014 surfaces of each sedimentary unit and the final surfaces in 2017.

The calculated net volume of eroded sediment for each sedimentary unit at each study site was divided by the planimetric (two-dimensional) area of the corresponding unit to estimate the net erosion per square meter. That value was divided by the study period duration (2.67 years) to estimate a normalized annual erosion rate (cubic meters per square meter per year).

At site 1 in the southwest corner of the Malakoff Diggins pit, three sedimentary units are exposed in a broad alcove. During the 2014–17 period, the three units produced a net total of 288±13 m^3 of sediment (tables 1 and 6), yielding an average erosion volume per unit area of 0.32±0.02 m^3/m^2. When computed on an annual basis, the surveyed area at site 1 yielded an erosion rate of 0.12±0.01 $m^3/m^2/yr$ (tables 1 and 6).

At study site 2 on the western margin of the Malakoff Diggins pit, six sedimentary units are exposed in a topographically complex amphitheater. The combined net erosion for all six units at site 2 totaled 3,283±154 m^3 (tables 2 and 6). Dividing by the total planimetric area (8,602 m^2) yielded an average erosion volume per unit area of 0.38±0.02 m^3/m^2. When computed on an annual basis, the imaged area at site 2 yielded an average erosion rate of 0.14±0.01 $m^3/m^2/yr$ (tables 2 and 6), the highest of the four sites surveyed.

Study site 4 is a 500-m-wide area along the northeast rim of the Malakoff Diggins mine pit and is composed of three separate cliff areas (western, central, and eastern). Correlation of the five mapped sedimentary units at site 4 to the lidar point cloud was only possible at the central and eastern areas. Consequently, the measured erosion of the sedimentary sequence in the western area was not differentiated. At study site 4, the combined net erosion for the western, central, and eastern areas totaled 8,517±145 m^3 (tables 3 and 6) and yielded an average erosion volume per unit area of 0.16±<0.01 m^3/m^2. The area-normalized annual erosion rate was 0.06±<0.01 $m^3/m^2/yr$ (tables 3 and 6) for the December 2014 to August 2017 period, the lowest of the four sites surveyed.

Site 5, located in the southeast corner of the Malakoff Diggins pit, has five sedimentary units exposed in two deeply dissected alcoves (eastern and western) that produced 846±22 m^3 of sediment during the December 2014 to August 2017 period (tables 4 and 6). Dividing the total net eroded volume (846±22 m^3) by the total planimetric area (3,293 m^2) yielded an erosion volume per unit area of 0.26±<0.01 m^3/m^2. When computed on an annual basis, the surveyed area at site 5 yielded an average erosion rate of 0.10±<0.01 $m^3/m^2/yr$ (tables 4 and 6).

The total net eroded volume documented with TLS for all four study sites from December 2014 to August 2017 was 12,934±334 m^3 (table 6) and the total planimetric surface area of the study sites was 65,777 m^3. The arithmetic mean of the erosion in cubic meters per square meter for the four study sites was 0.28 +0.10/–0.12 and the arithmetic mean of the erosion rate in cubic meters per square meter per year for the four study sites was 0.10±0.04 (table 6).

Horizontal retreat maps indicate that a variety of erosional processes were responsible for the net eroded sediment volume. These included areally broad and smaller scale processes such as persistent dry ravel, periodic sheet wash, and frost heave, as well as more localized and larger scale processes such as coalescing rill and gully erosion, debris flows, rotational landslides, and block-fall failures.

The results of this study will be combined with laboratory determination of grain-size distribution, mineralogy, and geochemistry of the various sedimentary units (Ward and others, 2019) to identify sources of sediment and metals within the pit that yield suspended sediment discharged from the pit through the Hiller Tunnel. Results from this investigation can be used by the State of California to facilitate the design of an effective sediment and heavy-metal abatement program for water discharged from the mine pit into Humbug Creek and to determine whether stabilization of sediment source areas could be needed at the Malakoff Diggins mine pit.

References Cited

California State Water Resources Control Board, 2017, Final 2014 and 2016 Integrated Report (Clean Water Act Section 303(d) List and 305(b) Report), accessed July 24, 2019, at https://www.waterboards.ca.gov/water_issues/programs/tmdl/integrated2014_2016.shtml.

Cassel, E.J., and Graham, S.A., 2011, Paleovalley morphology and fluvial system evolution of Eocene–Oligocene sediments ("auriferous gravels"), northern Sierra Nevada, California—Implications for climate, tectonics, and topography: Geological Society of America Bulletin, v. 123, nos. 9–10, p. 1699–1719, https://doi.org/10.1130/B30356.1.

Curtis, J.A., 2017, Geomorphic map of Malakoff Diggins State Historic Park, California: U.S. Geological Survey data release, https://doi.org/10.5066/F7ST7NQZ.

Fleck, J.A., Alpers, C.N., Marvin-DiPasquale, M., Hothem, R.L., Wright, S.A., Ellett, K., Beaulieu, E., Agee, J.L., Kakouros, E., Kieu, L.H., Eberl, D.D., Blum, A.E., and May, J.T., 2011, The effects of sediment and mercury mobilization in the South Yuba River and Humbug Creek confluence area, Nevada County, California—Concentrations, speciation, and environmental fate—Part 1: Field characterization: U.S. Geological Survey Open-File Report 2010–1325A, 95 p., https://doi.org/10.3133/ofr20101325A.

Heritage, G.L., and Large, A.R.G., eds., 2009, Laser scanning for the environmental sciences: Hoboken, N.J., Wiley-Blackwell, 278 p.

Howle, J.F., 2019, Terrestrial laser scanning data from Malakoff Diggins State Historic Park, Nevada County, California, 2014–17: U.S. Geological Survey data release, https://doi.org/10.5066/P9H3VNSN.

Howle, J.F., Alpers, C.N., Bawden, G.W., and Bond, S., 2016, Quantifying the eroded volume of mercury-contaminated sediment using terrestrial laser scanning at Stocking Flat, Deer Creek, Nevada County, California, 2010–13: U.S. Geological Survey Scientific Investigations Report 2015–5179, 23 p., https://doi.org/10.3133/sir20155179.

Howle, J.F., Alpers, C.N., Kitchen, J., Bawden, G.W., and Bond, S., 2019, Quantifying the eroded and deposited mass of mercury-contaminated sediment by using terrestrial laser scanning at the confluence of Humbug Creek and the South Yuba River, Nevada County, California, 2011–13: U.S. Geological Survey Scientific Investigations Report 2019–5104, 30 p., https://doi.org/10.3133/sir20195104.

Marvin-DiPasquale, M., Agee, J.L., Kakouros, E., Kieu, L.H., Fleck, J.A., and Alpers, C.N., 2011, The effects of sediment and mercury mobilization in the South Yuba River and Humbug Creek confluence area, Nevada County, California−Concentrations, speciation, and environmental fate—Part 2: Laboratory experiments: U.S. Geological Survey Open-File Report 2010–1325B, 53 p., https://doi.org/10.3133/ofr20101325B.

State of California, 2019, Public Resources Code (PRC), Division 5. Parks and monuments, Chapter 1.4. California Wild and Scenic Rivers Act (5093.50–5093.71), accessed July 24, 2019, at https://leginfo.legislature.ca.gov/faces/codes_displayText.xhtml?lawCode=PRC&division=5.&title=&part=&chapter=1.4.

Ward, A.J., Alpers, C.N., Campbell, K.M., Kane, T.J., Roth, D.A., Plowman, T.I., Antweiler, R.C., Monohan, C., Howle, J.F., Curtis, J.A., and Orlando, J., 2019, Geochemical, mineralogical, and grain-size data for in situ solid materials and suspended sediment at Malakoff Diggins State Historic Park, Nevada County, California: U.S. Geological Survey data release, https://doi.org/10.5066/P95RLMEI.

Glossary

Colluvial slope A general term for loose, unconsolidated sediments that have been eroded from a higher slope position (typically a steeper slope) and deposited down slope (typically on a lower angle slope) by gravity-driven processes.

Dry ravel A general term that describes the gravity-driven rolling, bouncing, and sliding of sediment particles down a slope.

Hydraulic gold mine A type of surface mine where a high-pressure jet of water (emitted from a water cannon or monitor) is used to dislodge or erode gold-bearing sedimentary deposits which are exposed on a hillside or cliff face.

Lidar (light detection and ranging) A remote-sensing technology used to make precise three-dimensional point clouds of the land surface. Pulses of near-infrared laser light are timed to measure the distance (range) from the laser scanner to the reflecting surface. Laser ranges are combined with angular orientation data to generate a dense and detailed set of points (locations of individual laser returns) referred to as a point cloud.

Point cloud A point cloud is a set of vertices in a three-dimensional coordinate system. These vertices are usually defined by x, y, and z coordinates and typically represent the external surface of an object.

Terrestrial laser scanning (TLS) Sometimes referred to as ground-based lidar or tripod-mounted lidar (T-lidar). The significance of ‘terrestrial’ refers to the laser scanner being near the Earth’s surface (stationary on a tripod) as opposed to airborne laser scanning (ALS).

Appendix Tables

Table 1–1. Malakoff Diggings study site 2 summary of net eroded volume of sedimentary units in the southern (S), western (W), and northern (N) areas from December 2014 to August 2017 and range of uncertainty, planimetric area of sedimentary units, erosion volume per unit area, and erosion rate.

[See figure 7 for the location of the various areas and extent of the sedimentary units. **Abbreviations**: m^3, cubic meter; m^2, square meter; m^3/m^2, cubic meter per square meter; $m^3/m^2/yr$, cubic meter per square meter per year; —, not applicable; ±, plus or minus]

Site 2 sedimentary unit	Net eroded volume (m^3)	Percentage of total eroded volume	Planimetric area of sedimentary unit (m^2)	Erosion volume per unit area (m^3/m^2)	Erosion rate ($m^3/m^2/yr$)
Southern area					
2A1-S	716	46	710	1.01	0.38
2B2-1-S	159	10	681	0.23	0.09
2B2-2-S	359	23	1,242	0.29	0.11
2C3-S	238	15	1,726	0.14	0.05
2D4-S	82	5	510	0.16	0.06
2D5-S	—[1]	—	—	—	—
Total for area	1,554	—	4,869	—	—
Average for area	—	—	—	[2]0.32	[3]0.12
Western area					
2A1-W	19	3	91	0.21	0.08
2B2-1-W	210	34	176	1.19	0.45
2B2-2-W	239	39	153	1.56	0.58
2C3-W	142	23	266	0.53	0.20
2D4-W	—[4]	—	—	—	—
2D5-W	—[5]	—	—	—	—
Total for area	610	—	686	—	—
Average for area	—	—	—	[2]0.89	[3]0.33
Northern area					
2A1-N	69	6	244	0.28	0.11
2B2-1-N	209	19	97	2.15	0.81
2B2-2-N	341	30	748	0.46	0.17
2C3-N	215	19	626	0.34	0.13
2D4-N	243	22	881	0.28	0.10
2D5-N	42	4	451	0.09	0.03
Total for area	1,119	—	3,047	—	—
Average for area	—	—	—	[2]0.37	[3]0.14

Table 1–1. Malakoff Diggings study site 2 summary of net eroded volume of sedimentary units in the southern (S), western (W), and northern (N) areas from December 2014 to August 2017 and range of uncertainty, planimetric area of sedimentary units, erosion volume per unit area, and erosion rate.—Continued

[See figure 7 for the location of the various areas and extent of the sedimentary units. **Abbreviations**: m^3, cubic meter; m^2, square meter; m^3/m^2, cubic meter per square meter; $m^3/m^2/yr$, cubic meter per square meter per year; —, not applicable; ±, plus or minus]

Site 2 area	Net eroded volume (m^3)	Percentage of total eroded volume	Total planimetric area (m^2)	Average erosion volume per unit area (m^3/m^2)	Average erosion rate ($m^3/m^2/yr$)
Site 2 areas combined					
Southern	1,554	47	4,869	0.32	0.12
Western	610	18	686	0.89	0.33
Northern	1,119	34	3,047	0.37	0.14
Site 2 - Total	3,283±154	—	8,602	—	—
Average net erosion	—	—	—	[2]0.38±0.02	[3]0.14±0.01

[1]Unit 2D5 not exposed in the southern area.

[2]The average erosion per unit area in cubic meters per square meter was calculated by dividing the total net eroded volume by the total planimetric area of the sedimentary units.

[3]The average erosion rate in cubic meters per square meter per year was calculated by dividing the average erosion per unit area in cubic meters per square meter by 2.67 years.

[4]Unit 2D4 in the western area had net deposition of 5 cubic meters—not used for erosion estimates.

[5]Unit 2D5 not exposed in the western area.

Table 1–2. Malakoff Diggings study site 4 summary of net eroded volume of sedimentary units in the central (C), eastern (E), and western areas from December 2014 to August 2017 and range of uncertainty, planimetric area of sedimentary units, erosion volume per unit area, and erosion rate.

[See figure 11 for the location of the various areas and figures 12–14 for the extent of the sedimentary units. **Abbreviations**: m^3, cubic meter; m^2, square meter; m^3/m^2, cubic meter per square meter; $m^3/m^2/yr$, cubic meter per square meter per year; <, less than; —, not applicable; ±, plus or minus]

Site 4 sedimentary units	Net eroded volume (m^3)	Percentage of total eroded volume	Planimetric area of sedimentary unit (m^2)	Erosion volume per unit area (m^3/m^2)	Erosion rate ($m^3/m^2/yr$)
Central area					
4A1-C	49	30	494	0.10	0.04
4A2-C	10	6	323	0.03	0.01
4A3-C	15	9	317	0.05	0.02
4A4-C	7	4	505	0.01	<0.01
4A5-C	82	51	299	0.27	0.10
Total for area	163	—	1,938	—	—
Average for area	—	—	—	[1]0.08	[2]0.03
Eastern area					
4A1-E	571	10	2,883	0.20	0.07
4A2-E	1,068	18	9,878	0.11	0.04
4A3-E	792	14	7,459	0.11	0.04
4A4-E	1,202	21	10,062	0.12	0.04
4A5-E	2,166	37	11,680	0.19	0.07
Total for area	5,799	—	41,962	—	—
Average for area	—	—	—	[1]0.14	[2]0.05

Site 4 area	Net eroded volume (m^3)	Percentage of total eroded volume	Total planimetric area (m^2)	Average erosion volume per unit area (m^3/m^2)	Average erosion rate ($m^3/m^2/yr$)
Site 4 areas combined					
Western	[3]2,555	30	9,095	0.28	0.10
Central	163	2	1,938	0.11	0.04
Eastern	5,799	68	41,962	0.12	0.04
Site 4 - Total	8,517±145	—	52,995	—	—
Average net erosion	—	—	—	[4]0.16±<0.01	[5]0.06±<0.01

[1]The average erosion per unit area in cubic meters per square meter was calculated by dividing the total net eroded volume by the total planimetric area of the sedimentary units.

[2]The average erosion rate in cubic meters per square meter per year was calculated by dividing the average erosion per unit area in cubic meters per square meter by 2.67 years.

[3]The sedimentary units in the western area were not differentiated.

[4]The average erosion per unit area in cubic meters per square meter was calculated by dividing the total net eroded volume by the total planimetric area of the sedimentary units.

[5]The average erosion rate in cubic meters per square meter per year was calculated by dividing the average erosion per unit area in cubic meters per square meter by 2.67 years.

Table 1–3. Malakoff Diggings study site 5 summary of net eroded volume of sedimentary units in the eastern areas 1 and 2 (E1, E2) and western areas 1 and 2 (W1, W2) from December 2014 to August 2017 and range of uncertainty, planimetric area of sedimentary units, erosion volume per unit area, and erosion rate.

[See figures 15–19 for the location and extent of the various areas and sedimentary units. **Abbreviations**: m^3, cubic meter; m^2, square meter; m^3/m^2, cubic meter per square meter; $m^3/m^2/yr$, cubic meter per square meter per year; —, not applicable; <, less than; ±, plus or minus]

Site 5 sedimentary units	Net eroded volume (m^3)	Percentage of total eroded volume	Planimetric area of sedimentary unit (m^2)	Erosion volume per unit area (m^3/m^2)	Erosion rate ($m^3/m^2/yr$)
			Eastern area 1		
5A1-E1	112	38	557	0.20	0.08
5A2-E1	50	17	82	0.61	0.23
5A3-E1	75	26	131	0.57	0.21
5A4-E1	38	13	246	0.15	0.06
5C5-E1	19	6	51	0.35	0.13
Total for area	294	—	1,067	—	—
Average for area	—	—	—	[1]0.27	[2]0.10
			Eastern area 2		
5A1-E2	78	40	138	0.56	0.21
5A2-E2	31	16	86	0.36	0.13
5A3-E2	50	26	181	0.28	0.10
5A4-E2	32	16	185	0.17	0.06
5C5-E2	4	2	67	0.06	0.02
Total for area	195	—	657	—	—
Average for area	—	—	—	[1]0.30	[2]0.11
			Western area 1		
5A1-W1	28	22	161	0.17	0.06
5A2-W1	26	20	77	0.34	0.13
5A3-W1	38	30	98	0.39	0.15
5A4-W1	27	21	126	0.21	0.08
5C5-W1	9	7	55	0.16	0.06
Total for area	128	—	517	—	—
Average for area	—	—	—	[1]0.24	[2]0.09
			Western area 2		
5A1-W2	56	24	388	0.14	0.05
5A2-W2	61	27	149	0.41	0.15
5A3-W2	48	21	124	0.39	0.15
5A4-W2	61	27	229	0.27	0.10
5C5-W2	3	1	162	0.02	0.01
Total for area	229	—	1,052	—	—
Average for area	—	—	—	[1]0.22	[2]0.08

Table 1–3. Malakoff Diggings study site 5 summary of net eroded volume of sedimentary units in the eastern areas 1 and 2 (E1, E2) and western areas 1 and 2 (W1, W2) from December 2014 to August 2017 and range of uncertainty, planimetric area of sedimentary units, erosion volume per unit area, and erosion rate.—Continued

[See figures 15–19 for the location and extent of the various areas and sedimentary units. **Abbreviations**: m^3, cubic meter; m^2, square meter; m^3/m^2, cubic meter per square meter; $m^3/m^2/yr$, cubic meter per square meter per year; —, not applicable; <, less than; ±, plus or minus]

Site 5 area	Net eroded volume (m^3)	Percentage of total eroded volume	Total planimetric area (m^2)	Average erosion volume per unit area (m^3/m^2)	Average erosion rate ($m^3/m^2/yr$)
Site 5 areas combined					
E1	294	35	1,067	0.28	0.10
E2	195	23	657	0.30	0.11
W1	128	15	517	0.25	0.09
W2	229	27	1,052	0.22	0.08
Site 5 - Total	846±22	—	3,293	—	—
Average net erosion	—	—	—	[1]0.26±<0.01	[2]0.10±<0.01

[1]The average erosion per unit area in cubic meters per square meter was calculated by dividing the total net eroded volume by the total planimetric area of the sedimentary units.

[2]The average erosion rate in cubic meters per square meter per year was calculated by dividing the average erosion per unit area in cubic meters per square meter by 2.67 years.

For more information concerning the research in this report, contact the
Director, California Water Science Center
U.S. Geological Survey
6000 J Street, Placer Hall
Sacramento, California 95819
https://ca.water.usgs.gov

Publishing support provided by the U.S. Geological Survey
Science Publishing Network, Sacramento Publishing Service Center

ISSN 2331-1258 (online)
https://doi.org/10.3133/ofr20191124